

1 FTIR-ATR & DFT STUDIES ON ADAPALENE 0.1%
2 AND BENZOYL PEROXIDE 2.5% GEL AND ITS
3 EFFICACY FOR THE TREATMENT OF ACNE
4 VULGARIS USING FTIR-ATR SPECTROSCOPIC
5 TECHNIQUE

6 Padmavathi R^{1*}, Rajamannan B², Gunasekaran S³, G. R. Ramkumar⁴, G. Sankari⁵, S. Muthu⁶

7 1 Department of Physics, Meenakshi Sundararajan Engineering College, Kodambakkam, Chennai, 600024,
8 TN, India; pathmavati@gmail.com

9 2 Engineering physics, FEAT Annamalai University, Annamalai Nagar, 608002, Chidambaram, TN, India.;
10 rajamannan1@gmail.com

11 3 Research and development St. Peter's institute of Higher Education and Research, St. Peter's
12 University, Avadi, Chennai, 600054, TN, India; deanresearchspu@gmail.com

13 4 Department of Physics, C. Kandaswaminaidu College for Men, Anna Nagar East, Chenna-600102, TN,
14 India; gr.ramkumar@yahoo.com

15 5 Department of Physics, Meenakshi College for Womens, Kodambakkam, Chennai-600024, TN, India;
16 gsankarik@gmail.com

17 6 Department of physics, Arignar Anna Govt.Arts College, Cheyyar-604407, TN, India,
18 mutgee@gmail.com

19
20 Correspondence; pathmavati@gmail.com

21
22 **Abstract:** FT-R –ATR spectra of gel Adapalene 0.1% and Benzoyl peroxide 2.5 % were recorded
23 and structural and spectroscopic data of the molecule in the ground state were calculated using
24 Hartee- Fock RHF/6-31G. The equilibrium geometry harmonic vibrational frequencies, infrared
25 intensities, Thermodynamic properties, HOMO-LUMO, Mulliken atomic charges, MEP were
26 calculated by Restricted Hartree-Fock RHF/ 6-31G basis set using Gaussian 09w program. The aim of
27 the present work is also to study the efficacy of the Gel ADP+BPO (Adapalene 0.1% & Benzoyl
28 Peroxide 2.5%) in the treatment of Acne vulgaris. Totally 20 subjects were studied to evaluate the
29 efficacy of gel ADP+BPO. 60 male and female subjects between the age group of 20-25 both healthy
30 subjects and acne affected were selected and single scalp hair tissues was collected. Hair is used to
31 detect acne vulgaris instead of analyzing blood to diagnose Acne Vulgaris, using FTIR-ATR
32 spectroscopic technique. The biomolecular changes in disease present in blood, hair, which looks like
33 blood, will also reflect the same biomolecular changes in the blood. FTIR spectra of the Acne hair
34 samples (post-treatment) were recorded in the mid-infrared region, and the biomarkers for the acne
35 vulgaris samples with specific peaks during the before treatment (pre) were analyzed and compared
36 along with, the hair samples of healthy subjects. The absorption values of some of the specific bands
37 of biomolecules present in the hair samples viz., protein, lipids, and squalene both the pre- and post-
38 treatment subjects are noted. The biomarkers are significantly different between pre- and post-

39 treatment hair samples of acne patients. Some of the biomarkers such as $R1 = I_{3264/2864}$, $R2 = I_{1633/2864}$,
40 $R3 = I_{1516/2864}$, and $R4 = I_{1454/2864}$ were used as diagnostic parameters, and hence the efficacy of
41 Adapalene 0.1% and Benzoyl Peroxide 2.5% is estimated. There is a significant difference between
42 pre and post treatment ($P < 0.05$, $P = 0.000$), There were no significant difference between healthy and
43 post treatment acne patients ($P > 0.05$, $P = 0.4290, 0.6040, 0.6160, 0.5070$).

44

45 **Keywords:** FTIR-ATR, Acne Vulgaris, Sebum, Sebaceous Glands, ADP+BPO, Squalene.

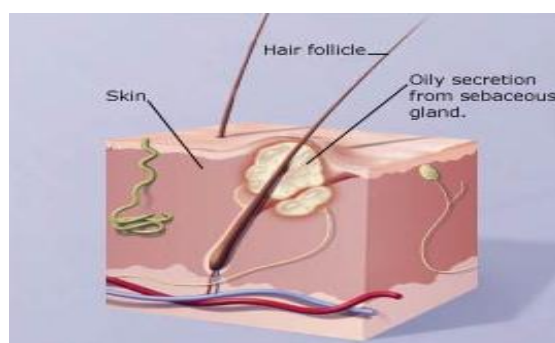
46

47

48 1. Introduction

49 Acne vulgaris is a chronic inflammatory disease of the pilosebaceous unit (comprising the hair
50 follicle and sebaceous gland) and is among the most common dermatological conditions worldwide,
51 with an estimated 650 million people affected Most people experience acne during adolescence, with
52 >90% of teenage boys and 85% of teenage girls affected [1,2]. Acne vulgaris is an exceptionally
53 common, recurring disease involving multiple etiological factors including follicular hyper
54 keratinization, increased sebum production, Propionibacterium acnes proliferation and
55 inflammation. It typically starts around the age of 15 to 20 years but tends to manifest earlier in female
56 patients. Scientist believe that increase in male hormones that are present in both males and feamles
57 lead to an over production of sebum.It occurs even in adults at the age of 25 to 45 years due to
58 hormonal disorders and genetic factor etc. It is also caused by inflammation of the hair follicles and
59 oil-producing (sebaceous) glands of the skin called pilosebaceous unit. Pilosebaceous density is
60 greatest on the face, upper neck, and chest and is roughly nine times the concentration found
61 elsewhere on the body. The sebaceous gland is attached to the upper third of the hair follicle as
62 shown in **Figure.1**, in the dermis layer. P.acnes is anaerobic bacteria, which means it cannot live in
63 the presence of oxygen. In addition to activating the immune system, studies show that P. acnes can
64 also activate groups of proteins called inflammasome complexes in the skin, which stimulate the
65 release of inflammatory molecules called cytokines. The human sebaceous glands do not achieve a
66 complete synthesis of Cholesterol and thus liberate pure squalene. Human sebum is dominantly
67 made up of triglycerides and fatty acids adding up to 57.5% of total lipids followed by wax esters
68 (26%), squalene (12%) and cholesterol (4.5%). The increased level of male hormones Androgens,
69 sebum lipid composition, P.acne overgrowth, and local pro-inflammatory cytokines drive epithelial
70 hyperproliferation. Although many acne vulgaris patients respond well to antibiotic drugs, there is
71 little relationship between the numbers of bacteria on the skin surface and the severity of acne.

72



73

Figure. 1 Hair Follicle

Based on expert consensus on relative effectiveness, the American Academy of Dermatology recommends doxycycline and minocycline (Minocin) rather than Tetracycline [3]. Kotori in his investigation, he found three months of treatment with low-dose isotretinoin (20 mg/d) was found to be effective in the treatment of moderate acne. Topical retinoids were indicated as monotherapy for non-inflammatory acne and as combination therapy with antibiotics to treat inflammatory acne. Adapalene (Differin) is the best-tolerated topical retinoid [4]. Several studies have been conducted to study the safety and efficacy of low-dose isotretinoin in the treatment of moderate to severe acne vulgaris [5, 3, 8, 6, 7, 8, and 9]. Doxycycline is a tetracycline antibiotic that fights bacteria in the body is used to treat many different bacterial infections, such as acne, urinary tract infections, intestinal infections, eye infections, gonorrhea, chlamydia, Periodontitis (gum disease), and others. These combinations can also improve patient compliance, increase the effectiveness of the treatment and decrease the development of bacterial resistance [10,11,12] have compared the efficacy and safety of 5% benzoyl peroxide, 0.1% adapalene, and their combinations. Topical retinoids, derivatives of vitamin A have been used to treat acne for almost three decades. Sebum of patients with acne contains lipoperoxide resulting from the peroxidation of the lipid squalene [13], lipoperoxides and MUFAS (Mono Unsaturated Fatty Acids) influence keratinocyte proliferation and differentiation, contributing to follicular hyperkeratinization [13, 14].

Topical retinoids, derivatives of vitamin A are the most effective comedolytic agents for the treatment of acne vulgaris by normalizing or even increasing the desquamation process, thereby decreasing the formation and the number of microcomedones. They also promote the clearing of pre existing comedones [15] and decrease in papulopustular lesions [16,17,18] Benzoyl peroxide and adapalene are among the most effective topical agents used in the treatment of acne vulgaris. Do Nascimento et al [19] compared the efficacy and safety of benzoyl peroxide 4% gel used twice daily with adapalene 0.1% gel used once daily they found benzoyl peroxide more effective than adapalane on noninflammatory and inflammatory lesions at weeks 2 and 5, and they found both drugs safe. Scientists hypothesize that one important factor is the way skin interacts with androgens in the bloodstream. The fatty acid content of sebum may play an important role in pore clogging, that fatty acids trigger the body's production of a specific inflammatory substance called Interleukin-1 (IL-1), which is known to trigger acne. ILs are groups of cytokines (secreted protein's and signal molecules) first seen by the white bloodcells (leukocytes).

To the best of our knowledge, molecular structure and analysis of the vibrational modes for the compound Adapalene (ADP) and Benzoyl peroxide (BPO) have not been performed using quantum chemical methods have not been performed. In the present work, FTIR-ATR spectra of ADP & BPO have been recorded and vibrational frequencies in the ground state has been calculated to distinguish fundamental modes from experimental vibrational frequencies and geometric parameters using ab initio HF methods and efficacy of the ADP 0.1% & BPO 2.5% also estimated using FTIR-ATR spectroscopic technique.

117

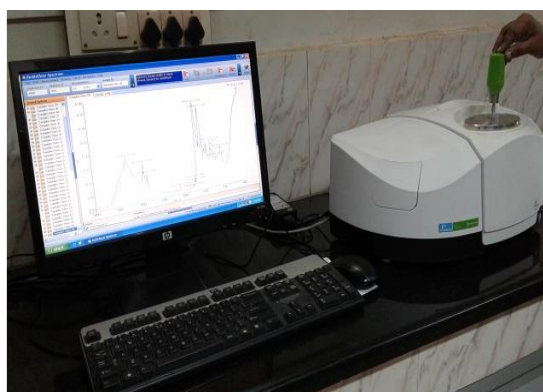
118 2. Materials and Methods

119

120 Twenty Acne vulgaris patients were introduced in the present investigation. All the 20 patients
121 were applied the combination topical gel adapalene 0.1% and benzoyl peroxide 2.5% (ADP+BPO)
122 daily on the night for one course of 3 months. After the 3 months treatment, single scalp hair samples
123 were collected from the patients (Post-treatment) and samples of single scalp hair samples were
124 obtained from 20 healthy subjects (control group) for FTIR-ATR spectral measurements. The samples
125 before medication of acne vulgaris patients were considered as the Pre-treatment samples. The
126 collected hair samples were subjected for FTIR-ATR spectral measurements were packed in an
127 airtight plastic cover stored away from heat and moisture. In order to eliminate any surface
128 contaminations, specimens were washed by dipping in distilled water for many times and the
129 washed hairs samples were admitted into laminar air flow to remove the water thoroughly, as water
130 is a good absorbent of infrared radiation, it affects the actual spectral response of the test material.
131 The hair samples collected were labelled with the respective subjects in a clean polyethene bags at
132 room temperature. The root end of the hair sample was placed on the internal reflectance crystal, and
133 force was applied by the pressure gauge on the hair sample to provide good optical contact with the
134 crystal. The FTIR-ATR spectra for all the samples were recorded in the mid-infrared region of
135 4000-450 cm^{-1} . Using Perkin Elmer Spectrum-Two FTIR Spectrophotometer having highly reliable and
136 single bounce diamond as its Internal Reflectance Element (IRE) as shown in the **Figure. 2**.

137

138



139

140

Figure. 2 FTIR-ATR Spectral recordings of Human Scalp hair tissues

141

142 The incident IR beam strikes the interface between the IRE and the sample of a lower refractive index.
143 Refractive index of the tissue sample hair in FTIR-ATR must be lower than the IRE employed.
144 Diamond is the IRE, which has a refractive index as 2.4, the Hair tissue have a refractive of 1.55, and
145 this enhances the spectra and gives detailed analysis of the tissue samples. This internal reflectance
146 creates an evanescent wave that extends beyond the surface of the crystal into the tissue sample held
147 in contact with the crystal. The FTIR-ATR spectra obtained are recorded at Sophisticated Analytical
148 Instrumentation facility (SAIF-SPIHER), St. Peter's Institute of Higher Education and Research, Avadi,
149 Chennai.

150

151

152 3. Treatment of Acne

153

154 Medicines in different forms like oral, ointment and tablets used as a treatment for acne often
155 effective alone in the mild to moderate acne and are important adjuncts to oral antibiotics in more
156 severe acne. The best-studied antibiotics include tetracycline and erythromycin. Other treatments like
157 Light and laser therapies can be used for the treatment of acne. Examples include visible light, pulsed-
158 dye laser, and photodynamic therapies. Overall, adapalene (Differin) is the best-tolerated topical
159 retinoid. Limited evidence suggests that tazarotene (Tazorac) is more effective than adapalene and
160 tretinoin (Retin-A). Adapalene 0.1% and Benzoyl peroxide 2.5 % Gel gel is a topical formulation
161 used for the treatment of different types of acne blackheads, whiteheads, cysts, nodules, and pustules,
162 which is an antibacterial skin-peeling agent.

163

- 164 ▪ the comedones are treated by topical tretinoin.
- 165 ▪ Mild inflammatory acne is treated by tropical retinoid like adapalene 0.1% + benzoyl
166 peroxide 2.5 % (ADP+BPO) as a combination therapy.
- 167 ▪ Moderate acne is treated with oral antibiotic plus topical therapy like tetracycline,
168 minocycline, erythromycin, and doxycycline.
- 169 ▪ Oral drug isotretinoin applies for severe acne, an oral treatment that needs to be taken
170 for 16 to 20 weeks.
- 171 ▪ Cystic acne may be treated with a corticosteroid injection called triamcinolone. This
172 injection into the lesion aims to reduce scarring caused by the inflammation.

173

174 The purpose of treatment for acne is for reducing sebum production, comedone formation,
175 inflammation, and bacterial counts and normalizing keratinization. Today's therapeutic modalities
176 for acne are aimed at one or more of its pathogenic precipitants, which include androgenic hormonal
177 stimulation, hypersecretion of sebum, faulty occlusion of the follicular orifice, P. acnes colonization,
178 and inflammation.

179

180 4. Adapalene:

181 Adapalene (ADP) is a newer topical retinoid used for the treatment of acne. It plays crucial role
182 by curing pimples on surface of the skin. ADP prevents breakouts, blackheads, whiteheads,
183 blemishes and clogged pores and restores skin tone and texture by clearing acne vulgaris. It reduces
184 the sebum level (LDL) squalene, lipids and unwanted proteins which causes acne. The IUPAC name
185 of adapalene is 6-[3-(1-adamantyl)-4-methoxyphenyl] naphthalene-2-carboxylic acid. Other names of
186 adapalene are Differin, Pimpal, Gallet, Adelene, and Adeferin. Its molecular mass is 412.52.g/mol. Its
187 chemical formula is $C_{28}H_{28}O_3$. Adapalene is a third-generation topical retinoid primarily used in the
188 treatment of mild-moderate acne, and is also used off-label to treat keratosis pilaris as well as other
189 skin conditions. It is effective against acne conditions where comedones are predominant.

190 Adapalene has a very low percutaneous absorption once the drug has penetrated the stratum
191 corneum, so that it becomes entrapped in the epidermis and hair follicle, which are targeted areas
192 [20]. Korkut and Piskin 2005 [21] demonstrated that adapalene is more effective in noninflammatory
193 lesions than inflammatory lesions. Adapalene 0.1% gel has been studied in 80 patients against
194 isotretinoin 0.05% gel, which is the cis-isomer of retinoic acid, to compare their effectiveness and

195 tolerance by [22]. **Dosik 2005** [23] compared the ability of the epidermis to tolerate adapalene 0.1%
196 cream and gel and tazarotene cream in concentrations of 0.05% and 0.1%. Topical treatments,
197 adapalene and benzoyl peroxide (BPO), are popular in mild-to-moderate acne vulgaris. With the
198 combined effect with BPO it retains its efficacy. **Brand et al. 2003** [24] demonstrated that 0.1%
199 adapalene and 5% benzoyl peroxide combination was safe and well-tolerated.

200

201 *4.1.1 Experimental*

202

203 The Compound Adapalene 0.1% is a gel was obtained from a leading Pharmaceutical and used
204 as such without further purification to record FTIR-ATR spectra. The FTIR spectrum of the title
205 molecule was recorded in the range 4000-450 cm^{-1} using FTIR-ATR technique with 4 cm^{-1} resolution
206 on Perkin Elmer Spectrum one FTIR spectrometer, recorded at Sophisticated Analytical
207 Instrumentation facility (SAIF-SPIHER), St. Peter's Institute of Higher Education and Research,
208 Avadi, Chennai.

209

210 *4.1.2 Computation*

211

212 To provide complete information regarding the structural characteristic and fundamental
213 vibrational modes of ADP, the Restricted Hartree-Fock and correlation functional calculations have
214 been carried out. The calculations of geometrical parameters in the ground state were performed
215 using Gaussian 03 programs [25]. The computations were performed at RHF/6-31G levels to obtain
216 the optimized geometrical parameters, vibrational wavenumbers of the normal modes, Mulliken
217 atomic charges, HOMO-LUMO, MESP and thermodynamical parameters of the compound. The
218 vibrational frequency assignments were made with a high degree of accuracy with the help of the
219 Chemcraft software program [26].

220

221 *4.1.3 Molecular Geometry*

222

223 The Title compound has 59 atoms with 171 normal modes of vibrations. The **Figure.3** shows the
224 optimized geometry of the molecule and **Table.1** represents the optimized values obtained for bond
225 lengths and bond angles and dihedral angles by RHF/6-3G basis set. The bond length between C31-
226 H59, C31-H58, C30-H57, C30-H56, C29-H55, C29-H54, C28-H53, C27-H52, C27-H51, C26-H50, C25-
227 H49, C25-H48, C24-H47, C23-H46, C23-H45, C21-H44, C21-H43, C21-H42 all have same bond length
228 of 1.113°. The bond length between C19-H41, C18-H40, C15-H39, C9-H37, C8-H36, C6-H35, C4-H34,
229 C3-H33, and C1-H32 have same value of 1.100°. The bond angle between O20-C21=1.40> C17-
230 O20=1.355> C11-O13= 1.338 > C11-O12= 1.208, these bond angle values are increase in order due to
231 the oxygen group present in the compound the sharing of electron between neighboring atoms occurs
232 easily which result in increased C-C bond length. The bond angle between H57-C30-C24, H57-C30-
233 C28 have same bond angle of 109.912°. The bond angle between C5-C10-C1, C1-C10-C9, H37-C9-C10,
234 H32-C1-C2, and C10-C1-C2 have the same bond angle of 120°. The bond angle between C19-C18-C17,
235 C14-C19-C18, H40-C18-C19, C19-C18-C17, C16-C15-C14, C7-C14-C19, H38-O13-C11 and O13-C11-O12
236 have the same bond angle of 119.999°. The dihedral angle between C17-C18-C19-H41, C20-C17-C18-
237 C19, C3-C2-C11-O13, O12-C11-O13-H38 and C16-C17-O20-C21 have same value of 180° respectively.

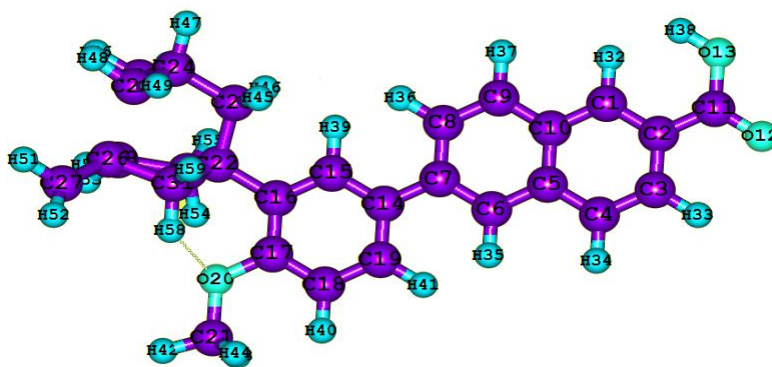


Figure. 3 The Atom numbering scheme of Adapalene

The dihedral angle between H32-C1-C10-C5, C8-C9-C10-C1 and C4-C5-C6-C7 the same value of -180° respectively. The dihedral angle is found to be zero for the C15-C14-C19-C18, C7-C14-C19-H41, C4-C5-C10-C1 and C2-C1-C10-C9 respectively.

4.1.4 Vibrational Assignments

The FTIR-ATR vibrational assignments of adapalene along with intensity and force constants and Raman activity are present in **Table.2**. The Experimental and Theoretical FTIR-ATR spectrum of adapalene is shown in **Figure. 4**. The aromatic CH stretching vibrations lie in the range of 3100-3000 cm^{-1} [27]. In the present investigation the computed CH stretching vibrations are occur at 3059, 3023, 3018, 2942, 2941, 2921, 2914, 2899, 2896, 2873, 2811, 2773 cm^{-1} in RHF/6-31G. The computed CH out-of-plane bending vibrations are assigned at 631, 620, 618, 609, 589, 567, 563, 540 cm^{-1} respectively. The CH_2 asymmetric stretching vibrations generally observed in the region 3000-2900 cm^{-1} . While the CH_2 symmetric stretching will appear in rage of 2900-2800 cm^{-1} . The computed CH_2 asymmetric vibrations occur at 3006, 2935 cm^{-1} in RHF/6-31G method and experimental value of FTIR occur at 2932 cm^{-1} . The CH_2 symmetric stretching vibrations occur at 2861 cm^{-1} in RHF/6-31G method. The Theoretical B3LYP wave numbers are in good agreement with experimental wavenumbers. The CH_2 in plane bending vibrations of RHF are assigned at 1677, 1670, 1664, 1663, 1660, 1653, 1646, 1639, 1635, 1627, 1606 cm^{-1} and experimental FTIR CH_2 occur at 1645, 1608 cm^{-1} . The computed CH_2 scissoring vibrations are occur at 1598, 1577, 1549, 1542, 1528, 1398, 1390, 1382, 1377, 1356 cm^{-1} in RHF/6-31G and experimental FTIR is occur at 1377 cm^{-1} . The experimental FTIR spectra 1455 cm^{-1} is assigned to CH_2 wagging, the corresponding RHF wavenumbers are 1496, 1492, 1486, 1476, 1463, 1433, 1429 cm^{-1} respectively. The computed CH_2 twisting bands are occur at 1356, 1353, 1346, 1341, 1319, 1306, 1292, 1281, 1264 cm^{-1} in RHF/6-31G and experimental FTIR occur at 1281 cm^{-1} . CH_2 torsion is assigned to 1244 cm^{-1} in FTIR, 1263, 1249, 1240, 1226, 1220, 726 cm^{-1} IN RHF. The computed CH_2 rocking vibrations are occur at 1056, 1054, 1042 cm^{-1} in RHF/6-31G. The out of plane bending vibrations of CH_2 in RHF are occur at 985, 880, 834, 820 cm^{-1} and experimental CH_2 837 cm^{-1} in FTIR respectively. The CH_3 vibrations of symmetric and asymmetric are appear in the region of 2962-2872 cm^{-1} [28] [43]. The calculated CH_3 asymmetric vibrations are occur at 3051, 2962 cm^{-1} in RHF/6-31G method and experimental value occur at 2972 cm^{-1} . The calculated symmetric CH_3 vibrations are occur at 2879, 2863 cm^{-1} and experimental value occur at 2878 cm^{-1} . The C=O vibrations are expected in the region 1850-1600 cm^{-1} . In the present study the

272 calculated C=O bands are occur at 1977, 1964, 1891, 1855, 1804, 1761, 1723, 1699, 1689, 1684,
 273 1019 cm^{-1} in RHF/6-31G and experimental FTIR values occur at 1923, 1698 cm^{-1} respectively. CO
 274 vibrations are occur in the region of 1260-1000 cm^{-1} . CO stretching vibrations of RHF are assigned at
 275 1263, 1249, 1220, 1219, 1202, 1196, 1137, 1135, 1076, 1072, 1056, 1054, 1036 cm^{-1} and experimental FTIR
 276 band occur at 1135 cm^{-1} . The Theoretical RHF C-O out-of-plane bending wavenumbers occur at 824,
 277 783, 653, 510, 486, 479 cm^{-1} and experimental FTIR band occur at 774, 473 cm^{-1} respectively. Socrates
 278 mentioned that the presence of conjugate substituent such as C=C causes a heavy doublet formation
 279 around the region 1625-1575 cm^{-1} . The calculated C=C wavenumbers are assumed at 1639, 1635, 1627,
 280 1606 cm^{-1} in RHF/6-31 G and experimental FTIR value occur at 1608 cm^{-1} . The bands 1430-1650 cm^{-1} in
 281 benzene derivatives are assigned to C-C stretching modes [29]. The six ring carbon atoms undergo
 282 coupled vibrations, called skeletal vibrations and give a maximum of four bands with the region
 283 1660-1220 cm^{-1} . In the present work, the computed C-C stretching vibrations are occur at 1598, 1577,
 284 1549, 1542, 1528, 1496, 1492, 1486, 1476, 1463, 1433, 1429, 1180, 1176, 1147, 1137, 1135, 1129, 1115, 1112,
 285 1103, 1086, 1076, 1072 803 cm^{-1} in RHF/6-31G FTIR value occur at 1455, 1135, 1078 cm^{-1} .

286
 287
 288

Table. 1 Optimized Geometrical parameters of Adapalene

S.NO	Parameter	RHF/6-31G	S.NO	Parameter	RHF/6-31G
1	C(31)-H(59)	1.113	38	C(26)-C(27)	1.523
2	C(31)-H(58)	1.113	39	C(25)-C(26)	1.912
3	C(30)-H(57)	1.113	40	C(24)-C(25)	1.523
4	C(30)-H(56)	1.113	41	C(23)-C(24)	1.523
5	C(29)-H(55)	1.113	42	C(22)-C(23)	1.523
6	C(29)-H(54)	1.113	43	C(17)-O(20)	1.355
7	C(28)-H(53)	1.113	44	O(20)-C(21)	1.402
8	C(27)-H(52)	1.113	45	C(14)-C(19)	1.337
9	C(27)-H(51)	1.113	46	C(18)-C(19)	1.337
10	C(26)-H(50)	1.113	47	C(17)-C(18)	1.337
11	C(25)-H(49)	1.113	48	C(16)-C(17)	1.337
12	C(25)-H(48)	1.113	49	C(15)-C(16)	1.337
13	C(24)-H(47)	1.113	50	C(14)-C(15)	1.337
14	C(23)-H(46)	1.113	51	C(2)-C(11)	1.351
15	C(23)-H(45)	1.113	52	C(11)-O(13)	1.338
16	C(21)-H(44)	1.113	53	C(11)-O(12)	1.208

17	C(21)-H(43)	1.113	54	C(5)-C(10)	1.337
18	C(21)-H(42)	1.113	55	C(1)-C(10)	1.337
19	C(19)-H(41)	1.100	56	C(9)-C(10)	1.337
20	C(18)-H(40)	1.100	57	C(8)-C(9)	1.337
21	C(15)-H(39)	1.100	58	C(7)-C(8)	1.337
22	O(13)-H(38)	0.972	59	C(6)-C(7)	1.337
23	C(9)-H(37)	1.100	60	C(5)-C(6)	1.337
24	C(8)-H(36)	1.100	61	C(4)-C(5)	1.337
25	C(6)-H(35)	1.100	62	C(3)-C(4)	1.337
26	C(4)-H(34)	1.100	63	C(2)-C(3)	1.337
27	C(3)-H(33)	1.100	64	C(1)-C(2)	1.337
28	C(1)-H(32)	1.100	65	H(59)-C(31)-H(58)	109.501
29	C(7)-C(14)	1.337	66	H(59)-C(31)-C(22)	109.481
30	C(16)-C(22)	1.497	67	H(59)-C(31)-C(26)	109.477
31	C(22)-C(31)	1.523	68	H(58)-C(31)-C(22)	109.453
32	C(26)-C(31)	1.523	69	H(58)-C(31)-C(26)	109.447
33	C(24)-C(30)	1.523	70	C(22)-C(31)-C(26)	109.469
34	C(28)-C(30)	2.038	71	H(57)-C(30)-H(56)	109.008
35	C(22)-C(29)	1.523	72	H(57)-C(30)-C(24)	109.912
36	C(28)-C(29)	1.523	73	H(57)-C(30)-C(28)	109.912
37	C(27)-C(28)	3.335	74	H(56)-C(30)-C(24)	109.634
75	H(56)-C(30)-C(28)	109.638	112	C(25)-C(24)-C(23)	109.468
77	H(55)-C(29)-H(54)	109.498	114	H(46)-C(23)-C(24)	109.480
78	H(55)-C(29)-C(22)	109.479	115	H(46)-C(23)-C(22)	109.473
79	H(55)-C(29)-C(28)	109.480	116	H(45)-C(23)-C(24)	109.454
80	H(54)-C(29)-C(22)	109.449	117	H(45)-C(23)-C(22)	109.452
81	H(54)-C(29)-C(28)	109.450	118	C(24)-C(23)-C(22)	109.472
82	C(22)-C(29)-C(28)	109.471	119	C(16)-C(22)-C(31)	109.469

83	H(53)-C(28)-C(30)	128.620	120	C(16)-C(22)-C(29)	109.473
84	H(53)-C(28)-C(29)	117.729	121	C(16)-C(22)-C(23)	109.474
85	H(53)-C(28)-C(27)	108.304	122	C(31)-C(22)-C(29)	109.471
86	C(30)-C(28)-C(29)	87.475	123	C(31)-C(22)-C(23)	109.468
87	C(30)-C(28)-C(27)	99.674	124	C(29)-C(22)-C(23)	109.473
88	C(29)-C(28)-C(27)	113.025	125	H(44)-C(21)-H(43)	109.519
89	H(52)-C(27)-H(51)	85.548	126	H(44)-C(21)-H(42)	109.467
90	H(52)-C(27)-C(28)	146.835	127	H(44)-C(21)-O(20)	109.459
91	H(52)-C(27)-C(26)	146.835	128	H(43)-C(21)-H(42)	109.445
92	H(51)-C(27)-C(28)	124.192	129	H(43)-C(21)-O(20)	109.438
93	H(51)-C(27)-C(26)	124.191	130	H(42)-C(21)-O(20)	109.499
94	C(28)-C(27)-C(26)	26.048	131	C(17)-O(20)-C(21)	120.005
95	H(50)-C(26)-C(31)	119.803	132	H(41)-C(19)-C(14)	119.995
96	H(50)-C(26)-C(27)	105.353	133	H(41)-C(19)-C(18)	120.006
99	H(50)-C(26)-C(25)	119.812	134	C(14)-C(19)-C(18)	119.999
98	C(31)-C(26)-C(27)	109.472	135	H(40)-C(18)-C(19)	119.999
99	C(31)-C(26)-C(25)	92.343	136	H(40)-C(18)-C(17)	120.002
100	C(27)-C(26)-C(25)	109.471	137	C(19)-C(18)-C(17)	119.999
101	H(49)-C(25)-H(48)	104.301	138	O(20)-C(17)-C(18)	119.995
102	H(49)-C(25)-C(26)	114.428	139	O(20)-C(17)-C(16)	120.002
103	H(49)-C(25)-C(24)	114.425	140	C(18)-C(17)-C(16)	120.003
104	H(48)-C(25)-C(26)	111.550	141	C(22)-C(16)-C(17)	120.002
105	H(48)-C(25)-C(24)	111.552	142	C(22)-C(16)-C(15)	119.996
106	C(26)-C(25)-C(24)	100.866	143	C(17)-C(16)-C(15)	120.002
107	H(47)-C(24)-C(30)	109.474	144	H(39)-C(15)-C(16)	120.003
108	H(47)-C(24)-C(25)	109.473	145	H(39)-C(15)-C(14)	119.998
109	H(47)-C(24)-C(23)	109.475	146	C(16)-C(15)-C(14)	119.999
110	C(30)-C(24)-C(25)	109.469	147	C(7)-C(14)-C(19)	119.999

111	C(30)-C(24)-C(23)	109.470	148	C(7)-C(14)-C(15)	120.003
149	C(19)-C(14)-C(15)	119.998	186	C(8)-C(7)-C(14)-C(15)	-1.153
150	H(38)-O(13)-C(11)	119.999	187	C(8)-C(7)-C(14)-C(19)	178.852
151	C(2)-C(11)-O(13)	120.004	188	C(15)-C(16)-C(22)-C(23)	-10.231
152	C(2)-C(11)-O(12)	119.998	189	C(15)-C(16)-C(22)-C(29)	109.774
153	O(13)-C(11)-O(12)	119.999	190	C(15)-C(16)-C(22)-C(31)	-130.227
154	C(5)-C(10)-C(1)	120.000	191	C(17)-C(16)-C(22)-C(23)	169.767
155	C(5)-C(10)-C(9)	119.998	192	C(17)-C(16)-C(22)-C(29)	-70.228
156	C(1)-C(10)-C(9)	120.000	193	C(17)-C(16)-C(22)-C(31)	49.771
157	H(37)-C(9)-C(10)	120.000	194	C(23)-C(22)-C(31)-C(26)	73.804
158	H(37)-C(9)-C(8)	119.995	195	C(23)-C(22)-C(31)-H(58)	-166.239
159	C(10)-C(9)-C(8)	120.005	196	C(23)-C(22)-C(31)-H(59)	-46.208
160	H(36)-C(8)-C(9)	120.005	197	C(29)-C(22)-C(31)-C(26)	-46.197
161	H(36)-C(8)-C(7)	120.005	198	C(29)-C(22)-C(31)-H(58)	73.761
162	C(9)-C(8)-C(7)	119.990	199	C(29)-C(22)-C(31)-H(59)	-166.208
163	C(14)-C(7)-C(8)	120.001	200	C(16)-C(22)-C(31)-C(26)	-166.197
164	C(14)-C(7)-C(6)	120.003	201	C(16)-C(22)-C(31)-H(58)	-46.239
165	C(8)-C(7)-C(6)	119.996	202	C(16)-C(22)-C(31)-H(59)	73.792
166	H(35)-C(6)-C(7)	120.003	203	C(25)-C(26)-C(31)-C(22)	-74.468
167	H(35)-C(6)-C(5)	119.999	204	C(25)-C(26)-C(31)-H(58)	165.570
168	C(7)-C(6)-C(5)	119.998	205	C(25)-C(26)-C(31)-H(59)	45.546
169	C(10)-C(5)-C(6)	119.998	206	C(27)-C(26)-C(31)-C(22)	173.920
170	C(10)-C(5)-C(4)	120.003	207	C(27)-C(26)-C(31)-H(58)	53.959
171	C(6)-C(5)-C(4)	119.997	208	C(27)-C(26)-C(31)-H(59)	-66.066
172	H(34)-C(4)-C(5)	120.005	209	H(50)-C(26)-C(31)-C(22)	52.176
173	H(34)-C(4)-C(3)	119.994	210	H(50)-C(26)-C(31)-H(58)	-67.786
174	C(5)-C(4)-C(3)	120.001	211	H(50)-C(26)-C(31)-H(59)	172.190
175	H(33)-C(3)-C(4)	120.007	212	C(23)-C(24)-C(30)-C(28)	60.191

176	H(33)-C(3)-C(2)	120.002	213	C(23)-C(24)-C(30)-H(56)	-179.961
177	C(4)-C(3)-C(2)	119.992	214	C(23)-C(24)-C(30)-H(57)	-60.158
178	C(11)-C(2)-C(3)	120.006	215	C(25)-C(24)-C(30)-C(28)	-59.802
179	C(11)-C(2)-C(1)	119.998	216	C(25)-C(24)-C(30)-H(56)	60.046
180	C(3)-C(2)-C(1)	119.996	217	C(25)-C(24)-C(30)-H(57)	179.849
181	H(32)-C(1)-C(10)	120.001	218	H(47)-C(24)-C(30)-C(28)	-179.804
182	H(32)-C(1)-C(2)	120.000	219	H(47)-C(24)-C(30)-H(56)	-59.956
183	C(10)-C(1)-C(2)	120.000	220	H(47)-C(24)-C(30)-H(57)	59.847
184	C(6)-C(7)-C(14)-C(15)	178.852	221	C(27)-C(28)-C(30)-C(24)	46.629
185	C(6)-C(7)-C(14)-C(19)	-1.143	222	C(27)-C(28)-C(30)-H(56)	-73.217
223	C(27)-C(28)-C(30)-H(57)	166.978	259	C(31)-C(26)-C(27)-C(28)	-118.893
224	C(29)-C(28)-C(30)-C(24)	-66.304	260	C(31)-C(26)-C(27)-H(51)	142.065
225	C(29)-C(28)-C(30)-H(56)	173.851	261	C(31)-C(26)-C(27)-H(52)	-8.164
226	C(29)-C(28)-C(30)-H(57)	54.046	262	H(50)-C(26)-C(27)-C(28)	11.180
227	H(53)-C(28)-C(30)-C(24)	169.580	263	H(50)-C(26)-C(27)-H(51)	-87.863
228	H(53)-C(28)-C(30)-H(56)	49.735	264	H(50)-C(26)-C(27)-H(52)	121.909
229	H(53)-C(28)-C(30)-H(57)	-70.070	265	C(24)-C(25)-C(26)-C(27)	-175.400
230	C(23)-C(22)-C(29)-C(28)	-85.457	266	C(24)-C(25)-C(26)-C(31)	72.988
231	C(23)-C(22)-C(29)-H(54)	154.582	267	C(24)-C(25)-C(26)-H(50)	-53.650
232	C(23)-C(22)-C(29)-H(55)	34.558	268	H(48)-C(25)-C(26)-C(27)	-56.847
233	C(31)-C(22)-C(29)-C(28)	34.540	269	H(48)-C(25)-C(26)-C(31)	-168.459
234	C(31)-C(22)-C(29)-H(54)	-85.421	270	H(48)-C(25)-C(26)-H(50)	64.904
235	C(31)-C(22)-C(29)-H(55)	154.555	271	H(49)-C(25)-C(26)-C(27)	61.257
236	C(16)-C(22)-C(29)-C(28)	154.538	272	H(49)-C(25)-C(26)-C(31)	-50.355
237	C(16)-C(22)-C(29)-H(54)	34.577	273	H(49)-C(25)-C(26)-H(50)	-176.992
238	C(16)-C(22)-C(29)-H(55)	-85.447	274	C(23)-C(24)-C(25)-C(26)	-69.519
239	C(27)-C(28)-C(29)-C(22)	-25.802	275	C(23)-C(24)-C(25)-H(48)	171.929
240	C(27)-C(28)-C(29)-H(54)	94.158	276	C(23)-C(24)-C(25)-H(49)	53.825

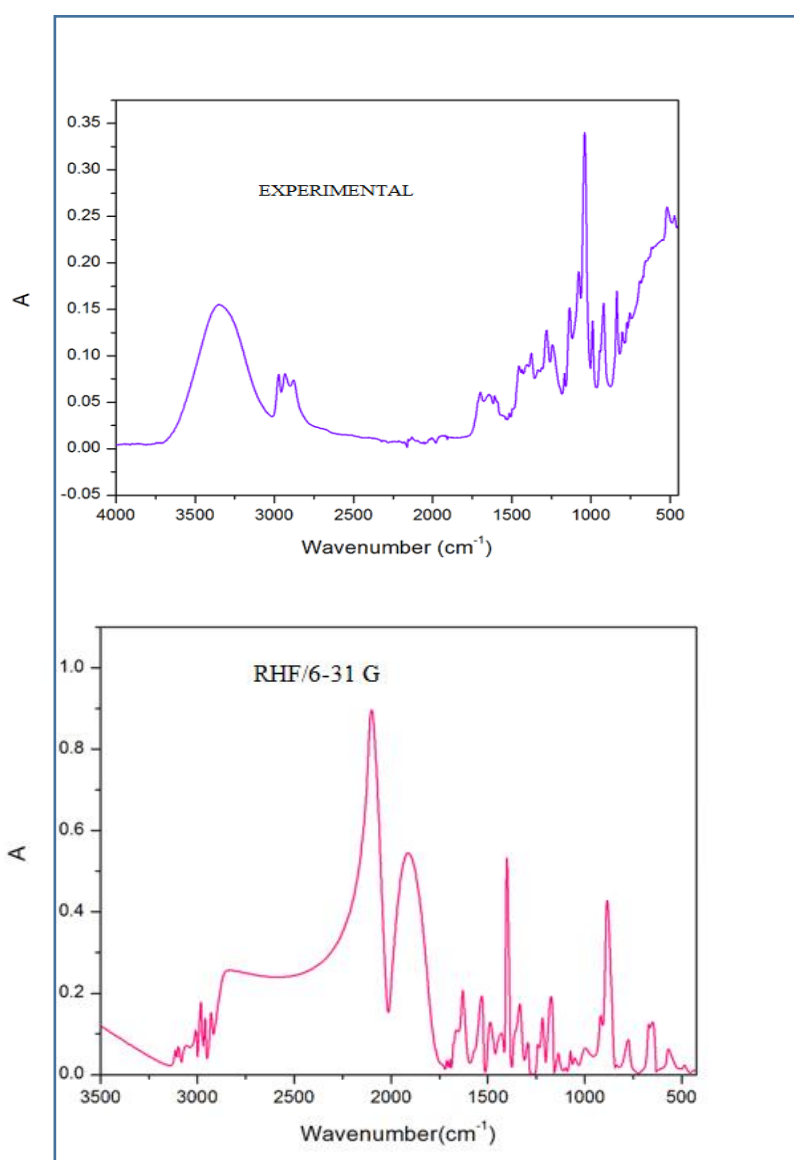
241	C(27)-C(28)-C(29)-H(55)	-145.817	277	C(30)-C(24)-C(25)-C(26)	50.476
242	C(30)-C(28)-C(29)-C(22)	73.638	278	C(30)-C(24)-C(25)-H(48)	-68.076
243	C(30)-C(28)-C(29)-H(54)	-166.402	279	C(30)-C(24)-C(25)-H(49)	173.820
244	C(30)-C(28)-C(29)-H(55)	-46.377	280	H(47)-C(24)-C(25)-C(26)	170.478
245	H(53)-C(28)-C(29)-C(22)	-153.313	281	H(47)-C(24)-C(25)-H(48)	51.926
246	H(53)-C(28)-C(29)-H(54)	-33.353	282	H(47)-C(24)-C(25)-H(49)	-66.177
247	H(53)-C(28)-C(29)-H(55)	86.673	283	C(22)-C(23)-C(24)-C(25)	62.904
248	C(26)-C(27)-C(28)-C(29)	47.628	284	C(22)-C(23)-C(24)-C(30)	-57.090
249	C(26)-C(27)-C(28)-C(30)	-43.741	285	C(22)-C(23)-C(24)-H(47)	-177.095
250	C(26)-C(27)-C(28)-H(53)	179.933	286	H(45)-C(23)-C(24)-C(25)	-57.062
251	H(51)-C(27)-C(28)-C(29)	146.668	287	H(45)-C(23)-C(24)-C(30)	-177.056
251	H(51)-C(27)-C(28)-C(30)	55.299	289	H(45)-C(23)-C(24)-H(47)	62.940
252	H(51)-C(27)-C(28)-H(53)	-81.027	290	H(46)-C(23)-C(24)-C(25)	-177.089
253	H(52)-C(27)-C(28)-C(29)	-63.101	291	H(46)-C(23)-C(24)-C(30)	62.917
254	H(52)-C(27)-C(28)-C(30)	-154.469	292	H(46)-C(23)-C(24)-H(47)	-57.088
255	H(52)-C(27)-C(28)-H(53)	69.205	293	C(29)-C(22)-C(23)-C(24)	62.794
256	C(25)-C(26)-C(27)-C(28)	141.262	294	C(29)-C(22)-C(23)-H(45)	-177.240
257	C(25)-C(26)-C(27)-H(51)	42.219	295	C(29)-C(22)-C(23)-H(46)	-57.218
258	C(25)-C(26)-C(27)-H(52)	-108.009	296	C(31)-C(22)-C(23)-C(24)	-57.206
297	C(31)-C(22)-C(23)-H(45)	62.761	334	C(3)-C(2)-C(11)-O(13)	180.000
298	C(31)-C(22)-C(23)-H(46)	-177.217	335	O(12)-C(11)-O(13)-H(38)	180.000
299	C(16)-C(22)-C(23)-C(24)	-177.202	336	C(2)-C(11)-O(13)-H(38)	-0.001
300	C(16)-C(22)-C(23)-H(45)	-57.235	337	C(4)-C(5)-C(10)-C(9)	179.426
301	C(16)-C(22)-C(23)-H(46)	62.786	338	C(4)-C(5)-C(10)-C(1)	0.000
302	C(16)-C(17)-O(20)-C(21)	180.000	339	C(6)-C(5)-C(10)-C(9)	-1.148
303	C(18)-C(17)-O(20)-C(21)	-0.004	340	C(6)-C(5)-C(10)-C(1)	179.426
304	C(17)-O(20)-C(21)-H(42)	-179.999	341	C(2)-C(1)-C(10)-C(9)	-179.426
305	C(17)-O(20)-C(21)-H(43)	-60.035	342	C(2)-C(1)-C(10)-C(5)	0.000

306	C(17)-O(20)-C(21)-H(44)	59.996	343	H(32)-C(1)-C(10)-C(9)	0.574
307	C(15)-C(14)-C(19)-C(18)	0.000	344	H(32)-C(1)-C(10)-C(5)	-180.000
308	C(15)-C(14)-C(19)-H(41)	-179.995	345	C(8)-C(9)-C(10)-C(1)	-180.000
309	C(7)-C(14)-C(19)-C(18)	179.995	346	C(8)-C(9)-C(10)-C(5)	0.574
310	C(7)-C(14)-C(19)-H(41)	0.000	347	H(37)-C(9)-C(10)-C(1)	-0.003
311	C(17)-C(18)-C(19)-C(14)	0.005	348	H(37)-C(9)-C(10)-C(5)	-179.429
312	C(17)-C(18)-C(19)-H(41)	180.000	349	C(7)-C(8)-C(9)-C(10)	0.574
313	H(40)-C(18)-C(19)-C(14)	-180.000	350	C(7)-C(8)-C(9)-H(37)	-179.424
314	H(40)-C(18)-C(19)-H(41)	-0.005	351	H(36)-C(8)-C(9)-C(10)	-179.425
315	C(16)-C(17)-C(18)-C(19)	-0.005	352	H(36)-C(8)-C(9)-H(37)	0.578
316	C(16)-C(17)-C(18)-H(40)	-180.000	353	C(6)-C(7)-C(8)-C(9)	-1.148
317	O(20)-C(17)-C(18)-C(19)	180.000	354	C(6)-C(7)-C(8)-H(36)	178.851
318	O(20)-C(17)-C(18)-H(40)	0.004	355	C(14)-C(7)-C(8)-C(9)	178.857
319	C(15)-C(16)-C(17)-C(18)	0.000	356	C(14)-C(7)-C(8)-H(36)	-1.144
320	C(15)-C(16)-C(17)-O(20)	179.996	357	C(5)-C(6)-C(7)-C(8)	0.574
321	C(22)-C(16)-C(17)-C(18)	-179.999	358	C(5)-C(6)-C(7)-C(14)	-179.431
322	C(22)-C(16)-C(17)-O(20)	-0.003	359	H(35)-C(6)-C(7)-C(8)	-179.424
323	C(14)-C(15)-C(16)-C(17)	0.005	360	H(35)-C(6)-C(7)-C(14)	0.572
324	C(14)-C(15)-C(16)-C(22)	-179.997	361	C(4)-C(5)-C(6)-C(7)	-180.000
325	H(39)-C(15)-C(16)-C(17)	-180.000	362	C(4)-C(5)-C(6)-H(35)	-0.003
326	H(39)-C(15)-C(16)-C(22)	-0.002	363	C(10)-C(5)-C(6)-C(7)	0.574
327	C(19)-C(14)-C(15)-C(16)	-0.005	364	C(10)-C(5)-C(6)-H(35)	-179.429
328	C(19)-C(14)-C(15)-H(39)	-180.000	365	C(3)-C(4)-C(5)-C(6)	180.000
329	C(7)-C(14)-C(15)-C(16)	-180.000	366	C(3)-C(4)-C(5)-C(10)	-0.574
330	C(7)-C(14)-C(15)-H(39)	0.005	367	H(34)-C(4)-C(5)-C(6)	0.003
331	C(1)-C(2)-C(11)-O(12)	-180.000	368	H(34)-C(4)-C(5)-C(10)	179.429
332	C(1)-C(2)-C(11)-O(13)	0.001	369	C(2)-C(3)-C(4)-C(5)	1.148
333	C(3)-C(2)-C(11)-O(12)	-0.001	370	C(2)-C(3)-C(4)-H(34)	-178.855

371	H(33)-C(3)-C(4)-C(5)	-178.851	376	C(11)-C(2)-C(3)-H(33)	-1.148
372	H(33)-C(3)-C(4)-H(34)	1.146	377	C(10)-C(1)-C(2)-C(3)	0.574
373	C(1)-C(2)-C(3)-C(4)	-1.148	378	C(10)-C(1)-C(2)-C(11)	-179.427
374	C(1)-C(2)-C(3)-H(33)	178.851	379	H(32)-C(1)-C(2)-C(3)	-179.426
375	C(11)-C(2)-C(3)-C(4)	178.853	380	H(32)-C(1)-C(2)-C(11)	0.573

289

290



291

292

293

294

295

296

Figure. 4 FTIR-ATR spectra of Adapalene

Table. 2 Observed and calculated frequencies of Adapalene

FTIR EXPT	Scaled freq	IR Intensity	Force constant	Raman Activity	Assignments
--------------	-------------	-----------------	-------------------	-------------------	-------------

3350	3685	2.6620	6.3956	127.2282	v OH
	3059	10.3663	6.2252	49.5107	v CH
	3051	39.1747	6.2216	25.4854	V _{asy} CH ₃
	3023	37.1678	5.9156	478.7435	v CH
	3018	23.0442	5.8946	62.9139	v CH
	3006	54.4630	5.9083	124.9968	V _{asy} CH ₂
2972	2962	40.5506	5.8330	98.4873	V _{asy} CH ₃
	2942	26.6545	5.7445	511.4049	v CH
	2941	98.9082	5.5978	301.8362	v CH
2932	2935	44.9350	5.7580	49.9770	V _{asy} CH ₂
	2921	39.5342	5.7394	48.6566	v CH
	2914	85.2315	5.4830	198.6996	v CH
	2899	33.6073	5.4420	102.9588	v CH
	2896	76.3543	5.3707	19.0849	v CH
2878	2879	55.0134	5.1866	106.7157	V _{sym} CH ₃
	2873	29.3165	5.3328	70.7639	v CH
	2863	118.9669	5.2932	314.8415	V _{sym} CH ₃
	2861	110.2095	5.0411	5516.3334	V _{sym} CH ₂
	2811	89.1802	17.6030	4179.6702	v CH
	2773	437.3359	19.7619	1237.8082	v CH
	1977	3.8746	12.9134	16.2597	v C=O
1923	1964	280.5847	13.1173	39.7310	v C=O
	1891	188.2628	5.6616	75.6184	v C=O
	1855	55.6235	4.4613	65.1191	v C=O
	1804	10.8446	3.8098	35.2173	v C=O
	1761	12.2709	4.3572	65.5086	v C=O
	1723	6.1336	2.0078	43.0515	v C=O
1698	1699	4.2949	1.9417	103.5844	v C=O
	1689	21.1845	4.1139	28.8214	v C=O
	1684	4.6147	1.8870	5.9800	v C=O
	1677	12.1995	2.4504	29.9063	δ CH ₂
	1670	12.5643	2.7034	9.3201	δ CH ₂
	1664	18.7515	1.8636	14.1049	δ CH ₂
	1663	6.7015	1.7761	28.8143	δ CH ₂
	1660	5.7883	1.9910	4.8676	δ CH ₂
	1660	37.7327	2.6489	27.1411	δ CH ₂
	1653	30.5500	2.5331	55.6484	δ CH ₂
1645	1646	55.5049	7.3253	8.9810	δ CH ₂
	1639	1.6501	1.8007	27.2554	δ CH ₂ + v C=C

	1635	34.7684	2.1606	19.6698	δ CH ₂ + ν C=C
	1627	124.6751	4.1979	26.5219	δ CH ₂ + ν C=C
1608	1606	3.7032	2.4844	0.5616	δ CH ₂ + ν C=C
	1598	15.9305	1.9064	28.2572	ω CH ₂ + ν CC
	1577	29.6270	1.9094	34.1139	ω CH ₂ + ν CC
	1549	21.1227	1.9759	18.2402	ω CH ₂ + ν CC
	1542	118.2264	2.6746	64.9448	ω CH ₂ + ν CC
	1528	12.3124	2.0587	3.5675	ω CH ₂ + ν CC
	1496	1.4617	2.5098	2.1430	ξ CH ₂ + ν CC
	1492	3.5079	2.3282	2.6659	ξ CH ₂ + ν CC
	1486	80.5533	1.9940	85.1203	ξ CH ₂ + ν CC
	1476	12.2884	1.8210	11.7624	ξ CH ₂ + ν CC
1455	1463	30.2041	1.7065	12.0019	ξ CH ₂ + ν CC
	1433	52.8917	1.6808	25.7336	ξ CH ₂ + ν CC
	1429	26.7350	1.5868	19.3509	ξ CH ₂ + ν CC
	1398	11.3834	1.6025	4.3956	ω CH ₂
	1390	316.7812	1.8016	17.8251	ω CH ₂
	1382	104.4757	2.5861	32.6045	ω CH ₂
1377	1377	11.1001	1.5613	15.7629	ω CH ₂
	1362	13.5201	1.5105	2.0954	τ CH ₂
	1356	0.8101	1.3733	5.5078	τ CH ₂ + ω CH ₂
	1353	45.9920	1.8180	1.5814	τ CH ₂ + ω CH ₂
	1346	48.0678	1.8849	113.0556	τ CH ₂ + ω CH ₂
	1341	96.5674	1.9731	423.3523	τ CH ₂ + ω CH ₂
	1319	11.6732	1.7272	6.6584	τ CH ₂ + ω CH ₂
	1306	15.5386	1.3884	22.9307	τ CH ₂ + ω CH ₂
	1292	46.7509	1.4205	131.5279	τ CH ₂
1281	1281	0.5006	1.2649	0.8103	τ CH ₂
	1264	0.9540	1.8473	2.8679	τ CH ₂
	1263	0.3803	1.2281	1.6700	ρ CH ₂ + ν CO
	1249	0.7783	1.1944	1.8952	ρ CH ₂ + ν CO
1244	1240	27.3214	1.8736	19.6378	ρ CH ₂ + ν CC
	1226	36.3977	1.3573	15.4118	ρ CH ₂ + ν CC
	1220	20.1959	1.2245	46.9899	ρ CH ₂ + ν CO
	1219	83.0639	4.3094	35.7691	ν CO
	1202	11.8293	1.4781	30.0260	ν CO

	1196	7.8191	1.6711	27.1782	vCC+vCO
	1180	123.6660	1.1251	3.7437	v CC
	1176	2.3422	1.0891	1.5378	v CC
	1147	0.9987	1.6278	1.9704	v CC
	1137	7.4005	2.3344	20.1367	v CC+v CO
1135	1135	23.6378	2.0446	21.3033	v CC+v CO
	1129	23.7399	1.0765	3.5798	v CC
	1115	6.3106	1.8891	18.1284	v CC
	1112	2.3727	1.4056	7.3874	v CC
	1103	10.1950	1.3525	74.4748	v CC
1078	1086	0.1336	0.9224	5.4378	v CC
	1076	12.2339	1.4369	12.4901	v CC+v CO
	1072	33.8430	1.0543	3.6678	v CC+v CO
	1056	3.0680	1.6447	22.1614	ξ CH ₂ + v CO
	1054	21.3515	0.8364	4.0562	ξ CH ₂ + v CO
1040	1042	13.7612	1.3133	21.3709	ξ CH ₂
	1036	5.4943	0.8824	3.9865	v CO + β CCC
	1019	35.5597	1.0172	27.2125	v C=O
990	1005	20.3339	1.5993	23.7498	τ HCCC
	985	19.1775	1.2216	18.1440	γ CH ₂
	954	24.8874	1.1707	25.3209	γ CH ₂
921	930	85.3905	1.4553	91.1173	β CCC
	909	13.7156	3.3215	7.7038	γ CH ₂
	902	277.1036	0.6739	9.0383	γ CH ₂
	880	1.0612	1.9337	5.1954	γ CH ₂
	871	8.9664	1.4958	20.7192	β CCC
837	834	10.8902	1.5352	292.9558	γ CH ₂
	824	5.8572	1.7368	410.9594	γ CO
	820	14.0979	1.9871	42.9006	γ CH ₂
	803	50.4882	2.2366	3.7163	v CC+ β CCC
774	783	9.0709	1.7938	5.1614	γ CO
755	756	3.4534	2.3590	0.4905	β HCCC
	750	0.0489	1.1020	4.4218	β HCCC
	726	6.4454	1.5630	16.9807	ρ CH ₂
	703	4.6818	0.7382	23.9018	β CCC
	690	66.1338	0.5726	9.3543	β CCC
	668	41.9708	0.7254	102.2525	β CCC
	658	70.0187	0.4605	8.0806	β CCC
	653	0.1140	1.3051	21.2514	γ CO
	631	4.4110	0.2676	0.3274	γ CH
	620	4.5099	0.6456	98.8306	γ CH

	618	7.5278	1.0000	10.8384	γ CH
	609	8.0799	0.5020	8.0575	γ CH
	589	33.7361	0.5992	7.4910	γ CH
	567	18.4863	0.7004	46.9722	γ CH
	563	11.8236	0.7128	31.2750	γ CH
	540	6.2908	0.8350	1.9299	γ CH
	524	7.8135	0.5403	15.8246	τ CCCC
519	517	4.3443	0.7836	23.4872	τ CCCC
	510	11.8076	0.4553	8.9849	γ CO
	486	7.8712	0.4049	23.6123	γ CO
473	479	3.1522	0.4228	142.0387	γ CO
	467	1.1041	0.4046	9.6769	τ CCCC
455	459	6.3096	0.5510	22.2597	β CCC
	442	1.2244	0.3261	6.0213	ν CC
	429	5.7684	0.2338	11.8234	ν CC
	392	9.5008	0.2897	140.7147	τ CCCC
	379	5.7903	0.2355	19.6944	τ CCCC
	315	1.1108	0.1775	7.0328	τ CCCC
	292	0.8433	0.0992	17.6512	β CCC
	246	8.2576	0.0512	39.8384	τ CCC
	185	0.6986	0.0600	6.1570	τ CCC
	150	8.2576	0.0512	39.8384	τ CCCC
	129	0.6986	0.0600	6.1570	τ CCCC
	86	11.3429	0.0156	2.3817	τ CCCC

297

298

299

300 **4.1.5 HOMO-LUMO**

301

302

303

304

305

306

307

308

309

310

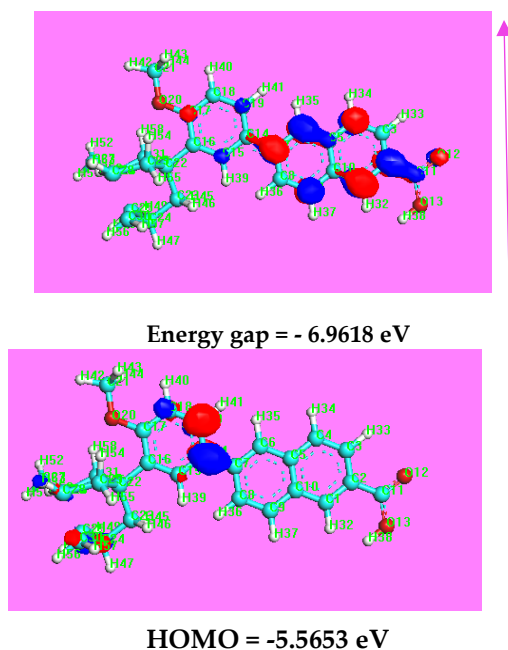
311

The highest occupied molecular orbitals (HOMOs) and the lowest unoccupied molecular orbitals (LUMOs) are called frontier molecular orbitals (FMOs). The HOMO represents the ability to donate an electron, LUMO determines the kinetic stability, chemical reactivity, and optical polarizability and chemical hardness-softness of a molecule. The HOMO represents the ability to donate an electron [30, 31, 32]. There are several ways to calculate the HOMO-LUMO energies. The energies of the HOMO is directly related to the ionization potential, LUMO energy related to the electron affinity.

$$\text{LUMO} = 1.3965 \text{ eV}$$

312

313



314

315

316

Figure. 5 3D plots of HOMO and LUMO of Adapalene

317

318 HOMO and LUMO orbital is called as energy gap that is important stability for the structure and
319 reveals the chemical activity of the molecule. The HOMO-LUMO energy gap calculated at RHF/
320 6-31G basis set and the title compound adapalene was illustrated in **Figure. 5**. The energy gap of
321 adapalene was found to be -6.9618 eV. The HOMO represents the ability to donate an electron whose
322 energy is calculated as -5.5653 eV and the LUMO as an electron acceptor represents the ability to
323 obtain an electron, LUMO energy is calculated as -1.3965 eV.

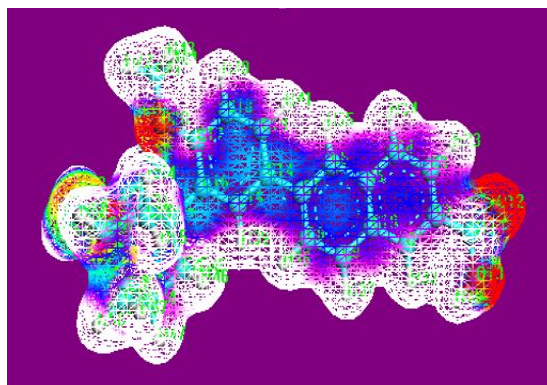
324

325 4.1.6 Molecular Electrostatic Potential

326 The molecular electrostatic potential (MESP) at a point in the space around a molecule gives
327 an indication of the net electrostatic effect produced at that point by the total charge distribution
328 (electron + nuclei) of the molecule and correlates with dipole moments, electronegativity, partial
329 charges chemical reactivity of the molecule. EPS surface, the positive electrostatic potential
330 corresponds to repulsion of the proton by atomic nuclei in regions where low electron density exists
331 and the nuclear charge is incompletely shielded represented in shades of blue. By definition, the
332 electron density iso-surface is a surface on which molecule's electron density has a particular value
333 and that encloses a specified fraction of the molecule's electron probability density. The potential
334 energy increases in the order of red < orange < yellow < green < blue. It provides a visual method to
335 understand the relative polarity of the molecule. While the negative electrostatic potential
336 corresponds to an attraction of the proton by the concentrated electron density in the molecule
337 represented in the shades of red on the coloring the iso surface with contours shows the electrostatic
338 potential at different points on the electron density isosurface. The electron density isosurface where
339 electrostatic potential surface has been mapped is shown in **Figure. 6**.

340

341
342
343
344
345
346
347
348
349
350



351 **Figure.6. Molecular Electrostatic Potential spectrum of Adapalene**

352
353
354
355
356
357
358
359

These electrostatic potential surface plots were obtained by Gauss View (Computer Prog). The different values of the electrostatic potential at the surface are represented by different colours: red represents regions of most negative electrostatic potential, blue represents region of most positive electrostatic potential and green represents regions of zero potential. The atoms O1, O2 and O3 are electrophilic reacting sites. The oxygen atoms indicates strongest repulsion. For the title molecule most positive electrostatic potential concentration was observed on the benzene and naphthalene.

360 4.1.7 Mulliken Atomic Charges

361
362
363
364
365
366
367
368

The oxygen atoms are electronegative characters, in ADP oxygen atoms O12, O13 and O20 have -0.5452, -0.7638 and -0.8081 respectively by RHF/6-31G method. The carbon atoms C11 and C17 are have high positive charges of 0.7855 and 0.4303 respectively. Except C11 and C17 all the other carbon atoms are have negative charges of C1 = -0.1051, C2 = -0.2067, C3 = -0.1427, C4 = -0.2089, C5 = -0.0567, C6 = -0.1145, C7 = -0.1479, C8 = -0.1540, C9 = -0.2084, C10 = -0.0703, C14 = -0.1525, C15 = -0.1360, C16 = -0.0296, C18 = -0.2641, C19 = -0.1157, C21 = -0.1403, C22 = -0.1280, C23 = -0.2822, C24 = -0.2361, C25 = -0.2223, C26 = -0.1652, C27 = -0.5052, C28 = -0.3259, C29 = -0.2747, C30 = -0.2642, C31 = -0.2771 and all the hydrogen atoms are have the positive charges and H38 has highest positive charge of 0.4537 and the net charges of hydrogen atom is 3.8040. The presence of negative charge on oxygen atoms and net +ve charge on hydrogen atoms may suggest the formation of intermolecular interactions in solid forms. The Milliken atomic charges obtained by RHF method are graphically represented for ADP in **Figure. 7** and values are tabulated in **Table.3**.

374

375 4.1.8 Thermodynamic Properties

376
377
378
379
380
381
382
383

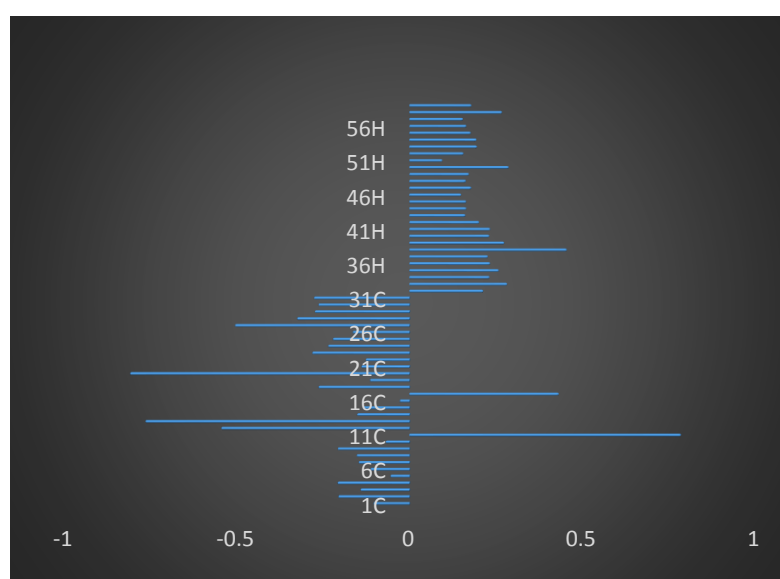
The zero point energy of Adapalene is calculated as 330.7742 Kcal/mol. Adapalene rotational constant and rotational temperature values are 0.3853, 0.0578 and 0.0523 its rotational temperature values are 0.0185, 0.0028 and 0.0025 respectively. ADP (Adapalene) total entropy value is calculated as 73.5610 (Cal/Mol/K), its total specific heat capacity is calculated as 124.0580 Cal/Mol/K and its total energy value is calculated as 340.6820 KCal/Mol respectively. Thermodynamic data's provide helpful information for further study on ADP. The total energy of Entropy, Enthalpy and specific heat capacity were also calculated and tabulated in the **Table 4**.

384
385
386
387

Table. 3 Mulliken Atomic Charges of Adapalene

S NO	Atoms	Charges									
1	C	-0.1051	18	C	-0.2641	34	H	0.2306	50	H	0.2858
2	C	-0.2067	19	C	-0.1157	35	H	0.2573	51	H	0.0943
3	C	-0.1427	20	O	-0.8081	36	H	0.2321	52	H	0.1551
4	C	-0.2089	21	C	-0.1403	37	H	0.2256	53	H	0.1941
5	C	-0.0567	22	C	-0.1280	38	H	0.4537	54	H	0.1929
6	C	-0.1145	23	C	-0.2822	39	H	0.2729	55	H	0.1764
7	C	-0.1479	24	C	-0.2361	40	H	0.2299	56	H	0.1634
8	C	-0.1540	25	C	-0.2223	41	H	0.2323	57	H	0.1536
9	C	-0.2084	26	C	-0.1652	42	H	0.2004	58	H	0.2663
10	C	-0.0703	27	C	-0.5052	43	H	0.1604	59	H	0.1783
11	C	0.7855	28	C	-0.3259	44	H	0.1635			
12	O	-0.5452	29	C	-0.2747	45	H	0.1630			
13	O	-0.7638	30	C	-0.2642	46	H	0.1487			
14	C	-0.1525	31	C	-0.2771	47	H	0.1776			
15	C	-0.1360	32	H	0.2122	48	H	0.1621			
16	C	-0.0296	33	H	0.2815	49	H	0.1711			

388
389
390



391
392
393
394

Figure. 7. Graphical representation of atomic charge distribution of ADP

395

Table. 4 Thermodynamic Properties of Adapalene

Parameters	RHF/6-31G	Parameters	RHF/6-31G
ZPVE (Kcal/Mol)	330.7743	Specific heat capacity(Cal/Mol /K)	124.058
Rotational constants(GHz)	0.3853	Translational	43.94
	0.058	Rotational	36.862
	0.0523	Vibrational	43.257
Rotational temperatures (Kelvin)	0.0185	Energy(KCal/Mol)	340.682
	0.0028	Translational	0.889
	0.0025	Rotational	0.889
Entropy(Cal/Mol/K)	73.561	Vibrational	338.904
Translational	2.981		
Rotational	2.981		
Vibrational	67.599		

396

397 **5. Benzoyl Peroxide:**

398 The IUPAC name of Benzoyl peroxide is Benzoyl benzenecarboperoxoate and its chemical
399 formula is $C_{14}H_{10}O_4$. Its molecular weight is 242.23 g/mol and its melting point is 217 to 221° F. It
400 place in isolation, out of the sunlight and away from heat. Sparingly soluble in water or alcohol,
401 vegetable oils [33]. It decomposes to release oxygen which kills acne producing bacteria. It has
402 bactericidal effect on Propioniumbacteria associated with acne, these bacteria induce antibiotic
403 resistance. Benzoyl peroxide also has been shown to decrease metabolism of sebaceous gland cells in
404 humans. Free fatty acids decrease in sebum of human patients treated with benzoyl peroxide,
405 presumably because of its antibacterial effect, as bacterial lipases are responsible for production of
406 free fatty acids. Benzoyl peroxide for acne treatment is applied to the affected areas in gel, cream, or
407 liquid, in concentrations of 2.5% increasing through 5.0%, and up to 10%. A small percentage of
408 people are much more sensitive to BPO and suffer from burning, itching, crusting and possibly
409 swelling. Applying the lowest concentration and building up as appropriate is most logical. Benzoyl
410 peroxide (BPO) was first made in 1905 and came into medical use in the 1930s. [29], it is on the World
411 Health Organization's list of Essential Medicines, the most effective and safe medicines needed in
412 a health system. Benzoyl peroxide is also believed to have a follicular flushing action [34]. By
413 applying on the skin, benzoyl peroxide is rapidly metabolized to benzoic acid, a harmless chemical.
414 Two common combination drugs include benzoyl peroxide/clindamycin and adapalene/benzoyl
415 peroxide an unusual formulation considering most retinoid are deactivated by peroxides. The main
416 advantage of benzoyl peroxide is that it clears blemishes fast by killing the acne-causing bacteria and
417 initially it was used just on affected areas because it would dry up the pimples very quickly. More
418 recently the ability of a BPO cleanser/wash formulation to reduce pre-existent antibiotic-resistant

419 P.acnes was evaluated [35, 36]. Clindamycin (CDP) + BPO showed an earlier onset of action with a
420 faster significant reduction in inflammatory and total lesion counts than Adapalene (ADA) [37].

421

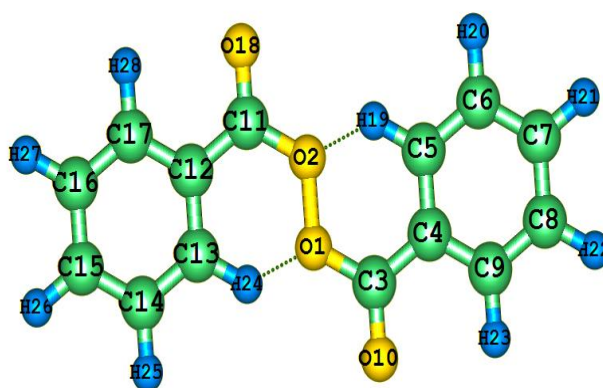
422 5.1.1 FT-IR Measurements

423 The gel Benzoyl peroxide 2.5% (BPO) was procured from a leading pharmaceutical and used as
424 such for recording FTIR-ATR spectrum. The FT-IR ATR spectrum of the gel BPO was recorded in the
425 range 4000-450 cm^{-1} using Perkin Elmer Spectrum Two FTIR-ATR spectrometer and shown in
426 **Figure 9**. The spectral measurements were carried out at SAIF, SPIHER, Avadi, Chennai.

427

428 5.1.2 Computational Details

429 The computational methods are an important tool in the characterization of more complex
430 molecules. Density functional theory (DFT) method is now standard in virtually all of the most
431 popular software packages. The most significant advantage to DFT method is significant with
432 increase in computational accuracy without additional increase in computing time. In the present
433 study the quantum chemical calculation has been performed using the Becke-3-Lee-Yang-Parr,
434 (B3LYP) supplemented with standard RHF/6-31G basis set using the Gaussian 09w program to
435 calculate the optimized geometry and vibrational numbers [38,39]. The calculated frequencies are
436 scaled by 0.97 for RHF/6-31G. The HOMO-LUMO, Mulliken atomic charges, thermodynamic
437 properties, MESP of the title compound were also performed using Gaussian 09w package program.
438 The optimized geometrical structure of BPO is shown in **Figure.8**.



439

440 **Figure.8. Optimized Structure and numbering of Benzoyl Peroxide**

441

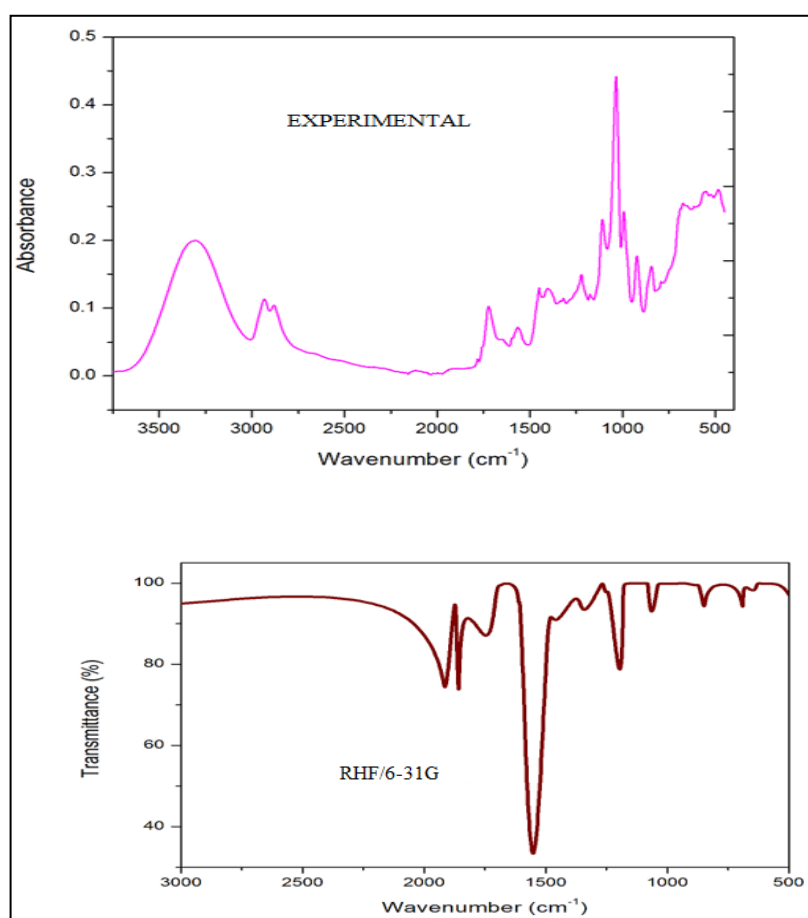
442 5.1.3 Vibrational Analysis

443 The title molecule consists of 28 atoms with 78 normal modes of vibrations. The observed FTIR
444 frequencies of Gel Benzoyl peroxide and calculated FTIR frequencies by DFT method values are
445 presented in the **Table.5**. The heteroaromatic organic compound and its derivatives are structurally
446 very close to benzene and commonly exhibit weak bands in the region 3100-3000 cm^{-1} due to C-H

447 stretching vibration. C-H stretching vibration is assigned to 2932, 2880 cm^{-1} in FTIR, the corresponding
448 RHF values are 2956, 2947, 2935, 2934, 2920 cm^{-1} respectively. The C-H in-plane bending vibrations in
449 the present study occur at 913, 898, 852, 842 cm^{-1} RHF basis set and experimental FTIR bands occur at
450 993, 922 cm^{-1} . The C-H out of plane bending vibrations in RHF are assumed 623, 612, 605, 604, 578, 516,
451 478 cm^{-1} and FTIR bands occur at 550, 483 cm^{-1} . The peroxide group vibrations have a weak absorption
452 band in the region of 900-800 cm^{-1} [40,41]. Due to O-O stretching vibration acid peroxides have strong
453 bands at range of 1820-1810 cm^{-1} . 1800-1780 cm^{-1} saturated aliphatic wavenumbers are due to their
454 C=O. For aryl bands occur in the region of 1805-1780 cm^{-1} and 1785-1755 cm^{-1} . The C=O stretching
455 vibrations occur at 1863, 1812, 1800, 1676 cm^{-1} in RHF/6-31G basis set and experimental FTIR band occur
456 at 1782, 1722 cm^{-1} respectively. C=O in-plane bending vibrations occur at 397, 293 cm^{-1} in RHF basis set.
457 The C-O stretching vibrations in FTIR is assigned 1109 cm^{-1} and the corresponding 1061 cm^{-1} in RHF
458 basis set and respectively. In the present investigation O-O stretching vibrations occur at 820, 668, 666
459 cm^{-1} in RHF 6-31G basis set and FTIR band assigned at 843, 673 cm^{-1} . The CC stretching vibrations are
460 observed in the region 1600-1400 cm^{-1} [42] for aromatic six membered rings e.g. benzene and
461 pyridines, there are two or three bands in this region due to skeletal vibrations.

462

463



464

465

466

467

468

Figure.9. FTIR-ATR Spectra of Benzoyl Peroxide

469
470
471

Table 5 Observed and calculated frequencies of Adapalene

Experimental Wavenumbers (cm ⁻¹)	Theoretical Scaled Wavenumbers RHF/6-31G	Red. masses	Force Constant	Assignment
	2956	1.1030	6.0372	v CH
	2947	1.0983	5.9723	v CH
	2935		5.8880	v CH
2932	2934	1.0904	5.8771	v CH
2880	2920	1.0834	5.7851	v CH
	1863	7.8826	17.1307	v C=O
	1812	6.8670	14.1240	v C=O
1782	1800	9.0326	18.3325	v C=O
1722	1676	2.5513	4.4881	v C=O
	1634	10.1681	16.9941	v C=C
	1564	2.9343	4.4942	v C=C
	1555	2.1698	3.2853	v C=C
1566	1508	2.0250	2.8854	v C=C
1450	1444	1.9248	2.5120	v C=C
1403	1432	2.0354	2.6129	v C=C
	1322	1.3739	1.5037	v C=C
	1313	1.3721	1.4819	v C=C
	1232	1.2388	1.1766	v C-C
	1230	1.0424	0.9880	v C-C
	1227	1.9292	1.8177	v C-C
	1214	1.5570	1.4367	v C-C
	1202	1.6017	1.4496	v C-C
	1153	2.8876	2.4037	v C-C
1109	1061	1.2221	0.8607	v C-O
	1048	1.3074	0.9000	v C-C
	1035	6.0310	4.0438	v C-C
1034	1007	1.3066	0.8302	v C-C
993	913	1.2334	0.6443	δ CH
922	898	14.0797	7.1022	δ CH
	852	7.0550	3.2074	δ CH
	842	6.4074	2.8416	δ CH
843	820	1.3030	0.5488	v OO
	681	7.4059	2.1524	δ CH
	669	5.1803	1.4538	δ CH
	668	6.9677	1.9478	v OO

673	666	5.6343	1.5627	ν OO
	623	8.4525	2.0534	γ CH
	612	7.3374	1.7201	γ CH
	605	4.0686	0.9340	γ CH
	604	4.0148	0.9183	γ CH
550	578	9.4159	1.9713	γ CH
	516	9.6918	1.6133	γ CH
483	478	10.1365	1.4486	γ CH
	382	9.9251	0.9075	δ C=O
	282	4.3542	0.2168	δ C=O
	278	3.9283	0.1896	γ CCC
	259	8.2932	0.3479	γ CCC
	255	3.8200	0.1550	γ CCC
	235	3.9453	0.1368	γ CCC
	184	4.8292	0.1024	δ OO
	50	5.2112	0.0080	γ CC

472

 ν – Stretching, δ – in plane bending; γ – out plane bending;

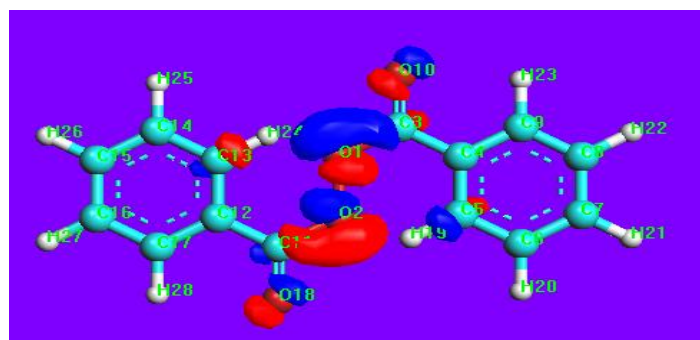
473

474

475

476

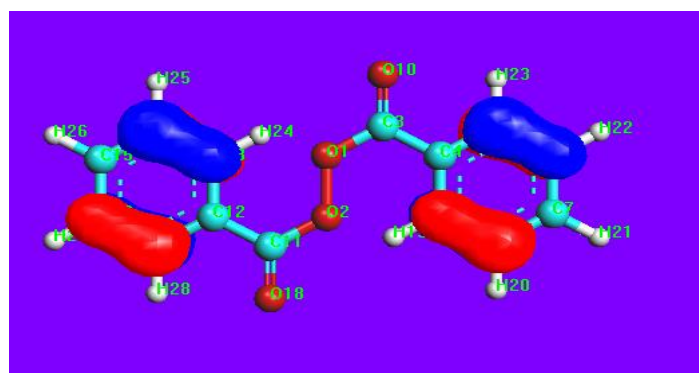
LUMO = -1.8403eV



477

478

Energygap= -11.6155 Ev



479

480

HOMO = -9.7752 eV

481

Figure . 10 HOMO and LUMO energy structure of BPO

482 The C=C stretching vibrations are occur in the region of 1600-1500 cm^{-1} . The C=C stretching vibrations
483 occur at 1634, 1564, 1555, 1508, 1444, 1432, 1322, 1313 cm^{-1} in RHF/6-31 G basis set and I FTIR band
484 occur at 1566, 1450, 1403 cm^{-1} respectively. The C-C stretching vibrations occur at 1232, 1230, 1227,
485 1214, 1202, 1153,1048,1035,1007 cm^{-1} in RHF/6-31G basis set and FTIR wavenumber occur at 1034 cm^{-1} .

486

487 5.1.4 HOMO-LUMO

488 The Highest Occupied Molecular Orbitals (HOMOs) and Lowest Unoccupied Molecular
489 Orbitals (LUMOs) are named as Frontier molecular orbitals (FMOs). The atomic orbital compositions
490 of frontier molecular orbitals are shown in **Figure. 10**. The LUMO as an electron acceptor represent
491 the ability to obtain an electron. The energy gap of HOMO-LUMO explains the eventual charge
492 transfer interaction within the molecule, which influences the biological activity of the molecule. The
493 positive and negative phases are represented in the red and blue colour respectively. The energy of
494 the two important Frontier Molecular Orbitals such as the highest occupied molecular orbital
495 (HOMO), the lowest unoccupied molecular orbital (LUMO) has been calculated. The energy value of
496 HOMO is -9.7752 eV and the energy value of LUMO is -1.8403 eV . The band gap between the HOMO
497 - LUMO is -11.6155 eV as calculated by RHF/6-31G basis set.

498

499 5.1.5 Thermodynamic Properties

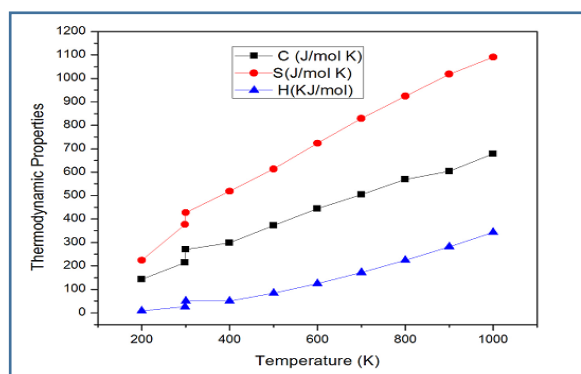
500 The standard thermodynamic parameters at room temperature such as zero-point vibrational
501 energy, therman energy, specific heat capacity, rotational constants and entropy of BPO were
502 calculated by RHF/6-31 Gbasis sets [43] and are listed in **Table. 6**. The Zero point energy is
503 calculated as 146.1067Kcal/Mol. The total entropy of BPO is 33.3020 Cal/Mol/K, the total Specific heat
504 capacity is calculated as 89.7670 Cal/Mol/ K and the total energy is calculated as 150.9780 Kcal/Mol
505 respectively. The variation of thermodynamic functional parameters with temperature is shown in
506 **Table 7**. The calculated entropy, specific heat capacity and enthalpy were found to be varied with a
507 positive temperature coefficient. When the temperature increased from 100 k to absolute temperature
508 298.15, the functional parameters are varied unhurriedly whereas from 350 to 100k temperature
509 coefficient, the thermodynamic functions seemed to swing in a linear pattern and were rather
510 constant at maximum temperatures. This variation shows the chemical hardness of the title
511 compound. The correlation between these thermodynamic properties and temperature are fitted by
512 quadratic formula as follows and corresponding fitting factors (R^2) for these thermodynamic

$$513 \quad S = -12.25868 + 0.87062 T - 1.88742 \times 10^{-4} T^2 \quad (R^2=0.99006)$$

$$514 \quad C_p = -35.87593 + 1.51784 T - 3.9296 \times 10^{-4} T^2 \quad (R^2=0.99485)$$

$$515 \quad \Delta H = -2.80392 + 0.01497 T + 3.3215 \times 10^{-4} T^2 \quad (R^2=0.99492)$$

516 properties were found to be 0.99006, 0.99485, and 0.99492. The temperature dependent
517 correlation graphs are shown in **Figure. 11**.



518

519

Figure. 11 Graphical Plot of BPO Thermodynamic Properties at various temperatures

520

Table. 6 Thermodynamic parameters of BPO

Parameters	RHF/6-31G	Parameters	RHF/6-31G
Zero point energy (Kcal/mol)	146.1067	Specific heat capacity (Cal/Mol/ K)	89.767
Rotational constants(GHz)	1.1889	Translational	42.353
	0.2354	Rotational	31.658
	0.1965	Vibrational	15.756
Rotational temperatures (Kelvin)	0.0571	Energy (KCal/Mol)	150.978
	0.0113	Translational	0.889
	0.0094	Rotational	0.889
Entropy (Cal/Mol/K)	33.302	Vibrational	149.201
Vibrational	27.34		
Translational	2.981		
Rotational	2.981		

521

522

523

Table.7 Thermodynamic properties of BPOat different temperature

524

525

526

527

528

529

530

T (K)	(S° _m) (J/mol K)	(C° _{pm}) (J/mol K)	(H° _m) (kJ/mol)
100	118.2	143	4.12
200	142.87	224.47	8.09
298.15	214.28	377.14	25.61
300	269.86	427.22	50.32
400	298.32	518.65	50.85

531 5.1.6 Mulliken Atomic Charges

532

533

534

The Mulliken atomic charges calculated by RHF method are shown in **Table 8**. The atomic charge in molecule is fundamental to chemistry. For instance, atomic charges has been used to

535 describe the processes of electronegativity equalization and charge transfer in chemical reactions, and
 536 to model the electrostatic potential outside molecular surface [44]. The electronegative atoms oxygen
 537 O1, O2, O10 and O18 shows negative charges of -0.5109, -0.5109, -0.5274 and -0.5274 respectively by
 538 RHF method. The carbon atoms C3 and C11 has maximum positive charges of 0.8621. Except C3 and
 539 C11 all other carbon atoms has negative charges of C4 = -0.3038, C5 = -0.0873, C6 = -0.2886, C7 =
 540 0.1545, C8 = -0.2560, C9 = -0.0862, C12 = -0.3038, C13 = -0.0873, C14 = -0.2886, C15 = -0.1545, C16 =
 541 -0.2560, C17 = -0.0862. The hydrogen atoms H19 and H24 are have maximum same positive charges
 542 0.4131 since they are attached to the Peroxide group of oxygen atoms and carbon atoms.

543
544
545
546 **Table. 8 Mulliken atomic charges of BPO**

547

S NO	Atoms	Charges	S NO	Atoms	Charges
1	O	-0.5109	15	C	-0.1545
2	O	-0.5109	16	C	-0.2560
3	C	0.8621	17	C	-0.0862
4	C	-0.3038	18	O	-0.5274
5	C	-0.0873	19	H	0.4131
6	C	-0.2886	20	H	0.2219
7	C	-0.1545	21	H	0.2216
8	C	-0.2560	22	H	0.2194
9	C	-0.0862	23	H	0.2765
10	O	-0.5274	24	H	0.4131
11	C	0.8621	25	H	0.2219
12	C	-0.3038	26	H	0.2216
13	C	-0.0873	27	H	0.2194
14	C	-0.2886	28	H	0.2765

548
549
550
551
552
553
554
555
556
557
558
559

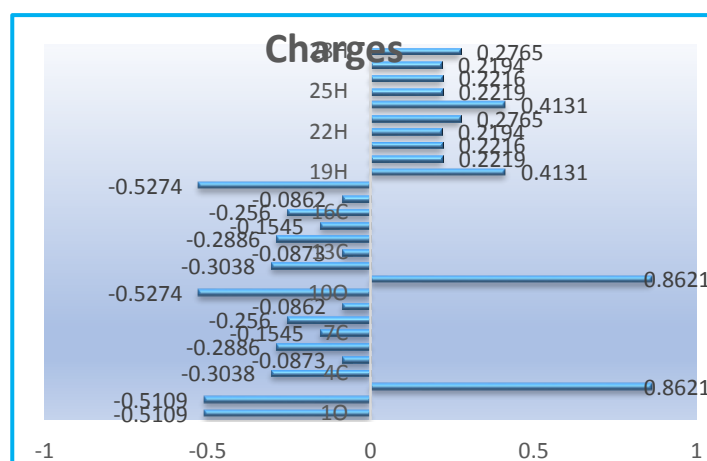
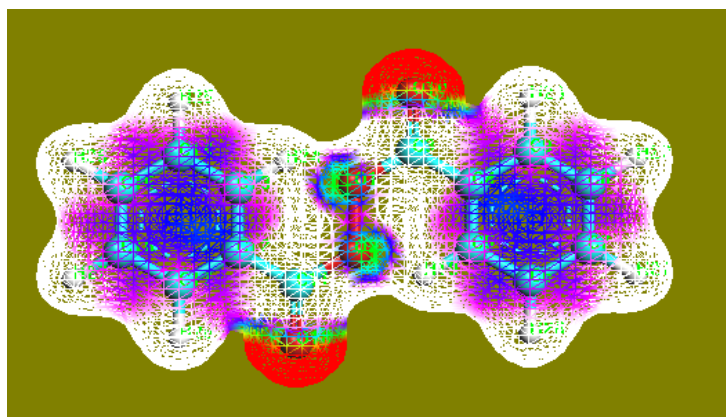


Figure. 12. Mulliken Charge distribution of Benzoyl Peroxide

562 From the above analysis, the presence of the higher charge on H19 and H24 atoms and the lower
563 charge on O2, O1 atom may suggest the formation of intramolecular interaction in solid forms. The
564 Mulliken Charge distribution of Benzoyl Peroxide is shown in **Figure.12**.
565

566 5.1.7 Molecular Electrostatic Potential

567 The molecular electrostatic potential surface of the molecule under study were constructed
568 using RHF/6-31G method using Gauss view 5.0 program is shown in **Figure 13**. The molecular
569 electrostatic potential surface is a useful quantity to explain hydrogen bindings, reactivity and
570 structural activity relationship of molecules including biomolecules and drugs [45, 46, 47]. The
571 different values of the electrostatic potential at the surface are represented by different colors; red
572 represents regions of most negative electrostatic potential, blue represents regions for most positive
573 electrostatic potential and green represents regions of zero potential. The atoms of oxygen atoms
574 O10 and O18 are electrophilic reacting sites, which indicates strongest repulsion, and the atoms O1
575 and O2 which are bonding with H1 and H6 and carbon atoms C8 and C1 shows less electrophilic
576 reacting sites, hence these oxygen atoms shows less repulsion effect. The two benzene rings shows
577 the most positive electrostatic potential respectively. From the MESP curve that the site
578 corresponding to the benzene ring is highly active and it play an important role in the activity of BPO,
579 whereas the sites corresponding to peroxide atoms is slightly active.



580

581 **Figure. 13. Molecular electrostatic potential surface of Benzoyl Peroxide**

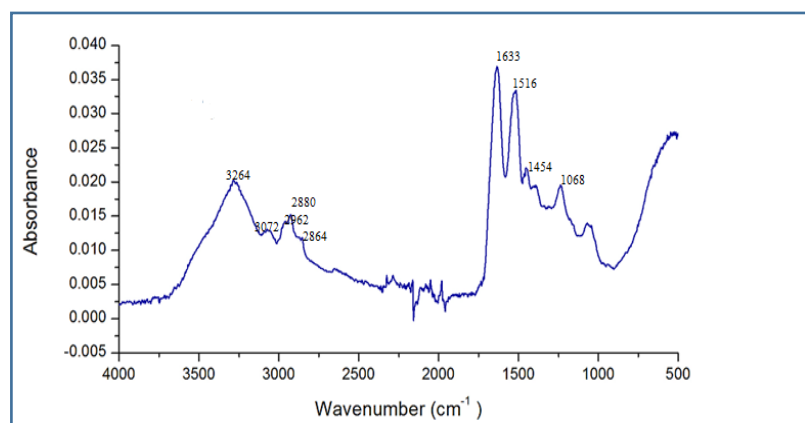
582

583 6. FTIR-ATR spectral profile of human scalp hair tissue

584

585 The FTIR-ATR spectral analysis undertaken in this investigation is mainly focuses on the
586 qualitative and quantitative as study of efficacy of acne vulgaris gel. The most important components
587 of hair are fibrous proteins (Keratins), melanin, glycogen, and lipids. Hair follicles are located 3-4 mm
588 below the capillary system. The biomolecular changes in the hair could be well examined using
589 molecular spectroscopic techniques. The FTIR-ATR absorption spectrum of healthy scalp hair is
590 represented in **Figure 14**. and the vibrational band assignments of the biomolecules of the human
591 hair fiber are shown in the **Table 9**. Vibrational band assignment is done with the idea of the group
592 frequencies of the various biomolecules present in the human scalp hair. The spectral region
593 3600-3000 cm^{-1} comprises of C-H, N-H and OH stretching modes of Amide (A) [48]. For the methyl
594 (CH_3) group of proteins and lipids are asymmetric and symmetric modes were observed at 2962 cm^{-1}
595 $^{-1}$ and 2864 cm^{-1} respectively, CH_2 for the methylene group of Fatty acids, the asymmetric mode

596 occurred at 2880 cm^{-1} [49]. The strong absorption band at 1633 cm^{-1} at corresponds to C=O stretching
 597 vibration coupled with an in plane bending of N-H and C-N stretching modes (Amide I band) [50].
 598 The vibration at 1516 cm^{-1} due to C=O stretching coupled with C-N stretching and bending
 599 deformation of N-H in the protein backbones [51]. The absorption in the keratin spectrum is
 600 attributed to the deformation and bending modes of the C-H/CH₂/CH₃ groups originating from the
 601 various amino acid (SC) side chains [52]. The bands are exemplified as medium, broad absorption at
 602 1454 cm^{-1} (LDL), while the band at 1245 cm^{-1} is due to asymmetric (PO₂) stretching vibrations of Lipid
 603 phosphate of amino acid [53]. The Spectral band at 1068 cm^{-1} is due to the contribution of C-O
 604 stretching vibrations of glucose.
 605
 606



607
 608 **Figure 14 Average FTIR-ATR Spectrum of healthy Human Scalp Hair tissue**

609

610 7. Discriminatin of Acne vulgaris Human Scalp Hair

611

612 FTIR absorption spectra of 20 healthy human scalp hair samples and 20 Acne hair human scalp
 613 hair samples were recorded. The spectral signatures of overlaid average spectra of healthy and acne
 614 vulgaris tissues are represented in **Figure 15**. The **Figure 15** emphasizes the difference in the intensity
 615 of IR absorption exhibited by the tissues; there is no spectral difference between the healthy and acne
 616 hair tissue samples with respect to wave numbers of various vibrational modes but considerable
 617 difference in the intensity of IR absorption of some specific vibrational modes of biomolecules
 618 present. The squalene main biomarker for acne vulgaris has occurred at 1454 cm^{-1} , whose absorption
 619 is high in acne patients when compared to healthy subjects.
 620

621 Ottaviani et al. 2010 the renowned researcher suggests the direct involvement of squalene
 622 peroxidation products on the onset of an inflammatory state in early acne lesions [54]. Hence the
 623 abnormalities in lipid and protein metabolism in acne are higher in above said, secretion of β -
 624 defensin and IL-8 protein and squalene (LDL) on target (i.e. hair) tissues. Among the lipid
 625 alterations, high-density lipoprotein (HDL) levels, which significantly decrease in patients with
 626 lesions, and the difference in the height of the histogram is important in the discrimination of acne
 627 vulgaris tissues from healthy subjects to LDL (low-density lipoproteins) levels. Which increase as the
 628 acne condition becomes more severe [55]. Based on these, vibrational bands observed at 3264 cm^{-1}
 629 (Protein), 1633 cm^{-1} (Amide I), 1516 cm^{-1} (Amide II), 1454 cm^{-1} (Squalene- LDL) have been considered
 630 as biomarkers for diagnosis of acne vulgaris.
 631
 632
 633
 634
 635
 636

637
638
639
640**Table 9 FTIR-ATR spectrum and vibrational analysis of biomolecules present in the human scalp Hair tissue**

Wavenumber (cm ⁻¹)	Band Assignment
3264	N-H stretching mode (Amide A) of Protein
3072	Amide –B band due to overtone of Amide I band
2962	Asymmetric stretching vibrations of CH ₃ of proteins and Lipids
2880	Asymmetric stretching vibrations of CH ₂ methylene group of fatty acids
2864	CH ₃ symmetric stretching of methane groups of proteins and Lipids
1633	C=O symmetric stretching vibrations of amide group Amide I
1516	Amide II band due to N-H bending vibration strongly coupled C-N stretching of Proteins
1454	δC-H/CH ₂ /CH ₃ of both lipid and protein groups (LDL), Squalene
1245	Asymmetric P=O stretching vibrations of PO ₂ stretching of Lipid Phosphate
1068	C-O stretching vibrations of glucose region

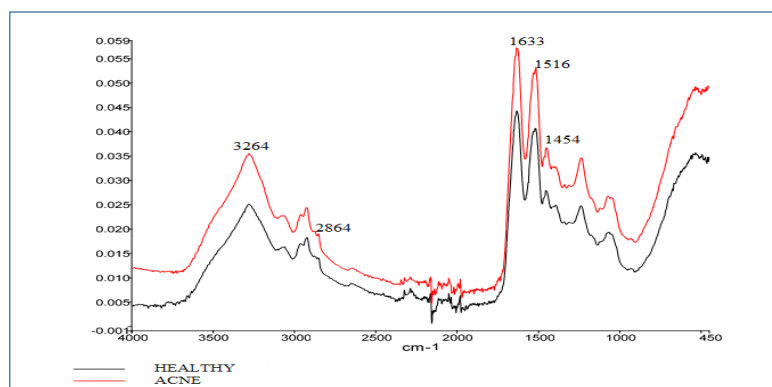
641
642

643 In order to get exact deviations and the intensity of absorption in the discrimination of acne vulgaris
644 from healthy tissues, internal parameter ratios are calculated. This deals with the ratio of the intensity
645 of infrared absorption of specific sensitive infrared bands. In acne patients, oxidative modification of
646 proteins, lipids, and nucleic acids been implicated in the mechanism of various diseases. Investigators
647 reported that components of sebum, particularly squalene, show enhanced comedogenicity when
648 oxidized [56]. Squalene is the biochemical precursor to the whole family of steroids and also which
649 is a precursor of cholesterol Indeed, squalene was reported to be highly sensitive to oxidation and
650 researchers reported that both squalene and its oxidized metabolites are found at much higher levels
651 in the acne vs. healthy [57]. Squalene is a triterpene of the general formula is C₃₀ H₅₀ that comprises 6
652 non-conjugated double bonds, making this compound one of the most unsaturated lipids.

653 From the pretreatment spectrum of the acne patients, it's viewed that, protein band which occurs
654 at 3264 cm⁻¹ is due to N-H stretching mode of (Amide A) of protein and the main absorption bands
655 are those associated with aliphatic C-H stretches of the saturated and unsaturated long chain fatty
656 acids, alcohols and esters. The asymmetric and symmetric stretching C-H vibrations of methane and
657 methylene groups belong to free fatty acids are found to be present around 2930-2873 cm⁻¹. The bands
658 occur at 2880 cm⁻¹ are belong to –CH₃ groups are due lipids and 1454 cm⁻¹ is due to –CH₂ scissoring
659 is due to squalene (LDL) [56].

660 The strong absorption band at 1633 cm⁻¹ at corresponds to C=O stretching vibration (Amide I)
661 whereas the amide II band centered around 1516 cm⁻¹ due to C=O stretching coupled with C-N
662 stretching and bending deformation of N-H in the protein backbone. The absorption in the keratin
663 spectrum are attributed to the deformation and bending modes of the C-H/CH₂/CH₃ groups
664 originating from the various amino acid (SC) side chains [52].

665
666



667
668
669
670
671
672
673

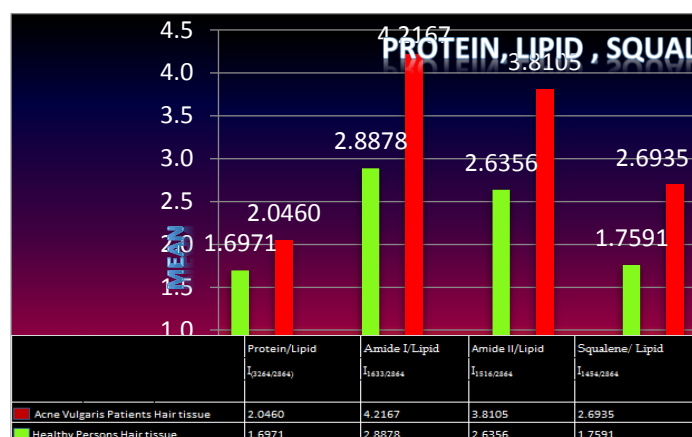
Figure 15 Overlaid Average FTIR-ATR Spectra of Healthy and Acne Vulgaris Human Scalp Hair tissues

Table 10 Intensity ratio parameters of Healthy and Acne Vulgaris tissues of Protein / Lipid, Amide I / Lipid, Amide II / Lipid and Squalene / Lipid

Samples	Protein / Lipid		Amide I / Lipid		Amide II / Lipid		Squalene / Lipid	
	I _{3264 / 2864}		I _{1633 / 2864}		I _{1516 / 2864}		I _{1454 / 2864}	
	Healthy	Acne Vulgaris						
1	1.9606	2.8254	3.5906	7.2222	3.3307	6.6508	2.1969	4.3968
2	1.7778	1.9606	2.963	3.6535	2.7099	3.3386	1.016	2.1732
3	1.6233	2.9211	2.214	6.9605	2.0605	6.3158	1.4186	4.3026
4	2.0000	2.0758	4.5606	4.2424	4.1364	3.7273	2.8485	2.6136
5	1.7241	2.2661	3.1724	5.2110	2.8793	4.6881	1.9052	3.3028
6	1.7711	2.2427	2.811	5.3786	2.607	4.8155	1.7662	3.2816
7	1.6933	1.7591	2.6626	3.4234	2.4601	3.0949	1.6503	2.1825
8	1.8571	2.0918	3.0357	5.2449	2.6929	4.7347	1.7786	3.2347
9	1.5848	1.8293	2.2712	3.0732	1.9915	2.6768	1.3051	1.8293
10	1.6418	1.7349	2.8806	2.9628	2.6119	2.7372	1.8060	1.7930
11	1.5773	1.7667	2.493	2.9528	2.2448	2.7444	1.6399	1.7922
12	1.7750	1.8122	2.975	2.9771	2.7875	2.7863	1.9000	1.9542
13	1.3119	2.1529	2.1835	3.9529	2.0367	3.6000	1.5688	2.4118
14	1.6310	1.7725	2.506	2.5059	2.2798	2.2797	1.5536	1.5536
15	1.6418	1.7035	2.8806	3.6627	2.6119	2.7209	1.806	2.5930
16	1.6340	1.6901	3.0825	3.7777	2.8041	3.4327	1.8763	2.6783
17	1.7238	2.0000	3.1429	4.1066	2.8952	3.8361	1.9429	2.5000
18	1.6995	2.0544	2.8653	3.9116	2.5959	3.4966	1.7668	3.2176
19	1.7407	2.4944	2.9722	5.4607	2.7315	5.0899	1.7963	3.3371
20	1.5734	1.7666	2.493	3.6527	2.2448	3.4444	1.6399	2.7222

674

675



676

677

678

679

680

681

682

683

684

685

686

687

688

689

690

691

Figure 16 Histogram Indicating the Mean Intensity Ratios of Healthy and Acne vulgaris Hair tissues of Protein/Lipid, AmideI/Lipid, Amide II / Lipid and Squalene / Lipid

692

8. Results and Discussion Efficacy of ADP+BPO

693

694

695

696

697

698

699

700

701

702

703

704

705

706

707

Internal parameter ignores the difference for sample under investigation, it nullifies the contradiction in the quantity of the sample and gives measured out exact deviation in the ratio of R_1 (3264/2864), R_2 (1633/2864), R_3 (1516/2864) and R_4 (1454/2864) of acne hair tissue. It is clear that, the absorption peaks of proteins and lipids for acne patients are more than the healthy person. The deviations in the internal ratio parameters of proteins and lipids of healthy and acne vulgaris tissues are provided clearly in **Tables 10**. For better understanding in deviation observed from internal ratio parameter calculations, the data obtained from internal ratio parameters is picturized-using histograms as shown in **Figure 16**. The histograms drawn between the ratios of Protein / Lipid, Amide I / Lipid, Amide II / Lipid and Squalene / Lipid shows the increase in height of the histogram of acne vulgaris. The statistical test was carried out for these four intensity ratio parameters.

Using the FTIR-ATR technique the spectral deviations are also identified very accurately for the Pretreatment and Post-treatment of the Acne vulgaris individuals. The average overlaid spectra of the hair samples of Pretreatment and Post treatment along with the healthy subjects are presented in the **Figure.17**. From the overlaid spectra, the absorption peaks of proteins (3264 cm^{-1}), Amide I (1633 cm^{-1}), Amide II (1516 cm^{-1}), and squalene (1454 cm^{-1}) are severe for the acne vulgaris patients when compare to healthy subjects because of the proteins, lipids, and squalene (LDL). From the **Figure.17** the band due to squalene at 1454 cm^{-1} absorption value in pretreatment has considerable difference when compared post treatment spectrum. The prominent absorption peak at 3264 cm^{-1} is due to protein band after post treatment with gel adapalene 0.1% and benzoyl peroxide 2.5% shows that absorption level is very well decreased. Amide I band 1633 cm^{-1} and Amide II band 1516 cm^{-1} absorption values also show difference in absorption levels after the post treatment. The sensitivity exhibited by the FTIR spectral bands of proteins, lipids due to the IR absorption of acne vulgaris tissue samples indicates that these were the key biomarkers in the investigation of acne vulgaris.

708

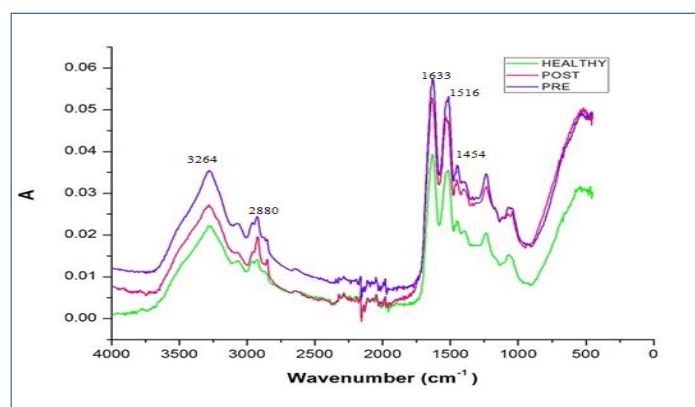


Figure. 17. The average overlaid FTIR-ATR spectra of Healthy, Pre and Post-treatment of Acne vulgaris patients Human Scalp Hair

709

710

711

712

713

714

9. Statistical Analysis

715

716

717

718

719

720

721

722

723

724

725

In the present investigation squalene, which is in the region 1454 cm^{-1} in the (Lipid) is the biomarker. The main aim is to control the level of protein, lipids, and squalene (LDL) present in the sebum. In order to find the efficacy of the Gel ADP+BPO in the treatment of acne vulgaris, the absorption values of the vibrational bands at 3264 , 1633 , 1515 cm^{-1} and 1454 cm^{-1} corresponding to protein, lipids, amide I, amide II, squalene (LDL) peaks respectively on (After 3 month course) spectra were noted. Biomarkers for acne vulgaris samples with specific peaks (Proteins/ lipids), (Amide I/lipids), (Amide II/lipids), (squalene /lipids) and the intensity ratio parameters were calculated. The significance of the intensity ratio results was estimated using dependent t-test statistic method. For the statistical interpretation, the low p-value ($p < 0.05$) is taken as statistically significant.

726

The efficacy is found out from the formula,

727

$$\% \text{ of Efficacy} = [A_{\text{Pre}} - A_{\text{Post}} / A_{\text{Pre}}] * 100$$

728

729

730

731

732

733

734

735

736

737

738

739

740

741

742

743

and the results were tabulated in **Table 11**. The FTIR spectral data were statistically analyzed by paired sample t-test for pre and post-treatment of the tissue samples. The mean and the standard deviation for pre and post treatment on the acne vulgaris individuals tissue samples were found from the above said four intensity ratio parameters Viz., $R_1 = I_{(3264/2864)}$, $R_2 = I_{(1633/2864)}$, $R_3 = I_{(1516/2864)}$ and $R_4 = I_{(1454/2864)}$ have been introduced and calculated for Pre and Post- Treatment. Acne vulgaris hair tissue samples and are given in **Table.12** and similarly the mean and the standard deviation for healthy and post-treatment acne on the acne vulgaris patients individuals tissue samples were found from the above said four intensity ratio parameters are presented in the **Table.13** respectively. The results obtained for the tissue samples from the statistical analysis by t-test shows that the pre and post-treatment mean values for the ratios $R_1 = I_{(3264/2864)}$ mean value have changed from 2.0460 to 0.7190, $R_2 = I_{(1633/2864)}$ mean value changes from 1.2506 to 0.0311, $R_3 = I_{(1516/2864)}$ mean value changes from 4.2167 to 1.7859 and $R_4 = I_{(1454/2864)}$ mean value changes from 2.6935 to 1.0057. The histogram with a comparison of the mean intensity Ratio Parameters of

744
745**Table.11 Intensity ratio parameters of pre and post treatment and Efficacy**

Samples	Stages	R ₁ = I ₃₂₆₄ (Proteins)/ I ₂₈₆₄ (Lipids)	R ₂ = I ₁₆₃₃ (AmideI)/ I ₂₈₆₄ (Lipids)	R ₃ = I ₁₅₁₆ (Amide II)/ I ₂₈₆₄ (Lipids)	R ₄ = I ₁₄₅₄ (Squalene)/ I ₂₈₆₄ (Lipids)
1	Pre	2.8254	7.2222	6.6508	4.3968
	Post	0.7761	2.449	3.8878	1.6429
	% of Efficacy	72.53 %	66.09 %	41.54 %	62.63 %
2	Pre	1.9606	3.6535	3.3386	2.1732
	Post	0.3893	1.1409	1.5711	0.2013
	% of Efficacy	80.14	68.77	52.94	90.73
3	Pre	2.9211	6.9605	6.3158	4.3026
	Post	2.0703	4.1094	3.6953	1.5859
	% of Efficacy	41.09	40.96	41.49	63.14
4	Pre	2.0758	4.2424	3.7273	2.6136
	Post	0.0094	0.8447	1.5031	0.441
	% of Efficacy	99.54	80.08	59.67	83.12
5	Pre	2.2661	5.211	4.6881	3.3028
	Post	1.0816	1.3776	2.1224	1.0306
	% of Efficacy	52.27	73.56	54.72	68.79
6	Pre	2.2427	5.3786	4.8155	3.2816
	Post	0.9857	2.5571	2.3143	0.4071
	% of Efficacy	56.04	52.45	51.94	87.59
7	Pre	1.7591	3.4234	3.0949	2.1825
	Post	0.4634	1.8976	0.7707	0.9024
	% of Efficacy	73.65	44.56	75.09	58.65
8	Pre	2.0918	5.2449	4.7347	3.2347
	Post	0.5071	2.0071	2.0500	0.1214
	% of Efficacy	75.75	61.73	56.79	96.24
9	Pre	1.8293	3.0732	2.6768	1.8293
	Post	0.7459	1.2486	1.1271	0.4530
	% of Efficacy	59.22	59.37	57.89	75.23
10	Pre	1.7349	2.9628	2.7372	1.7930
	Post	0.3390	1.3631	1.0446	1.0210
	% of Efficacy	80.45	53.99	61.83	43.05
11	Pre	1.7667	2.9528	2.7444	1.7922
	Post	0.1077	1.3385	1.0692	1.0077
	% of Efficacy	93.90	54.67	61.04	43.77
12	Pre	1.8122	2.9771	2.7863	1.9542
	Post	1.0000	1.3681	1.0123	1.0552
	% of Efficacy	44.81	54.04	63.66	46.00
13	Pre	2.1529	3.9529	3.6000	2.4118

	Post	0.8854	1.9167	1.6823	0.8750
	% of Efficacy	58.87	51.51	53.26	64.72
14	Pre	1.7725	2.5059	2.2797	1.5536
	Post	0.4583	1.4722	1.0000	0.6944
	% of Efficacy	74.14	41.25	56.13	55.30
15	Pre	1.7035	3.6627	2.7209	2.5930
	Post	0.1412	1.2040	1.5028	1.4181
	% of Efficacy	91.71	67.12	44.76	45.31
16	Pre	1.6901	3.7777	3.4327	2.6783
	Post	1.0014	1.0408	1.7041	1.5408
	% of Efficacy	40.74	72.44	50.35	42.47
17	Pre	2.0000	4.1066	3.8361	2.5000
	Post	1.1418	2.1560	1.7518	1.4052
	% of Efficacy	42.91	47.49	54.33	43.79
18	Pre	2.0544	3.9116	3.4966	3.2176
	Post	1.0048	1.7762	1.3762	1.3714
	% of Efficacy	51.09	54.59	60.64	57.37
19	Pre	2.4944	5.4607	5.0899	3.3371
	Post	1.0163	3.0976	2.6748	1.6260
	% of Efficacy	59.25	43.27	47.44	51.27
20	Pre	1.7666	3.6527	3.4444	2.7222
	Post	0.2562	1.3518	1.3577	1.3139
	% of Efficacy	85.49	62.99	60.58	51.73

746
747
748

Table. 12 Mean Intensity Ratio Parameters Pre and Post Treatment Acne Vulgaris Patients using t-test

IRP Ratios	Pre Treatment			Post Treatment			t	p
	N	Mean	SD	N	Mean	SD		
Protein/Lipid I _{3264/2864}	20	2.0460	0.3584	20	0.7190	0.4826	15.7230	0.0000
AmideI/Lipid I _{1633/2864}	20	4.2167	1.3056	20	1.7859	0.7901	12.1790	0.0000
Amide II/Lipid I _{1516/2864}	20	3.8105	1.2124	20	1.7609	0.8468	19.8950	0.0000
Squalene/Lipid I _{1454/2864}	20	2.6935	0.7971	20	1.0057	0.4873	10.1230	0.0000

749
750
751
752
753
754

Healthy, Pre, and Post-treatment of Acne Vulgaris individuals Hair Samples are shown in **Figure.18**. There is a statistically significant difference in levels of proteins, lipids, and squalene, for each of the internal ratio parameters R1-R4. From the **Table.12**, the low p-value ($p < 0.05$) indicates that there is a significant difference between the means of the internal ratio parameters calculated for pre and post-treatment hair tissue samples, and hence there is discrimination

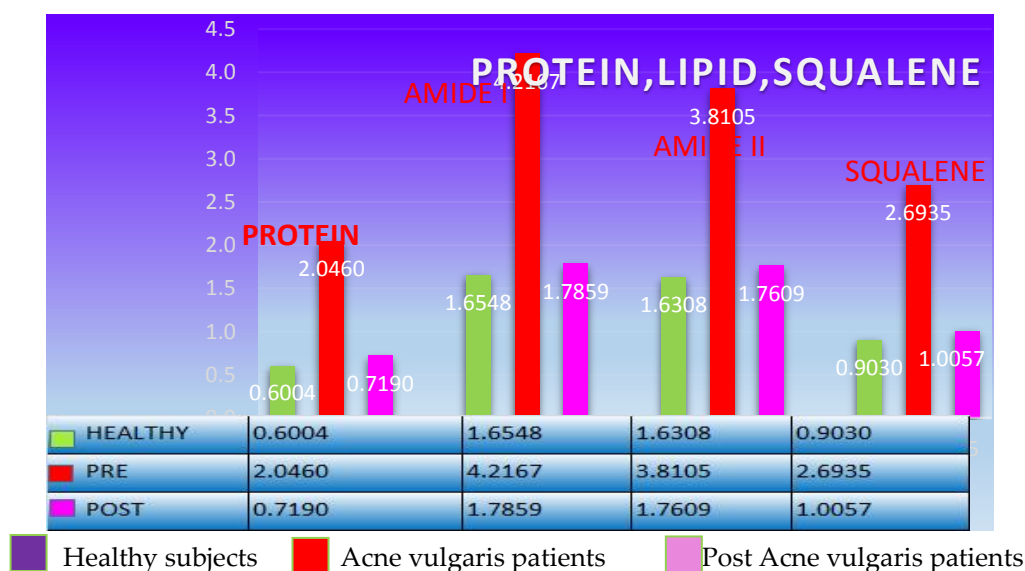
755

756

Table. 13 Mean Intensity Ratio Parameters of Healthy and Post Treatment Acne Vulgaris Patients - t-test

IRP Ratios	Healthy			Post Treatment			t	p
	N	Mean	SD	N	Mean	SD		
Protein/Lipid I _{3264/2864}	20	0.6004	0.4567	20	0.7190	0.4826	0.7990	0.4290
Amide I/Lipid I _{1633/2864}	20	1.6548	0.7943	20	1.7859	0.7901	0.5230	0.6040
Amide II/Lipid I _{1516/2864}	20	1.6308	0.7774	20	1.7609	0.8468	0.5060	0.6160
Squalene/Lipid I _{1454/2864}	20	0.9030	0.4831	20	1.0057	0.4873	0.6690	0.5070

757



758

759

760

761

762

Figure. 18. Histogram indicating the mean intensity ratio parameter of healthy subjects,**Pre and Post Treatment of Acne vulgaris patient's Human scalp hair tissues**

763 between Pre and Post-treatment have been thus proved from this statistical method and hence stands

764 as an evidence for method adopted. From the **Table.13**, the p-value ($p > 0.05$) indicates that there is

765 no difference between Healthy subjects and post-treatment respectively, therefore almost a better

766 results occur between the means of the internal ratio parameters calculated for post-treatment human

767 scalp hair tissue and healthy subjects as evidence.

768

769 **10. Conclusion**

770

771 Density functional theory calculations have been carried out on the structure and vibrational

772 spectra of Adapalene and Benzoyl peroxide. The equilibrium geometry computed by DFT level for

773 both bond length and bond angles are performed better. The vibrational frequencies analysis by

774 RHF/6-31G method agree satisfactorily with experimental results. HOMO-LUMO energy gap helped

775 in analyzing the chemical reactivity of the molecule. The Energy gap in ADP and BPO <1.30 explain
776 about both were highly reactive and stable. Mulliken charge distribution of the molecule were studied
777 by RHF method indicated the electronic charge distribution in the molecule. MEP showed the
778 different negative and positive potential sites of the molecule in accordance with the total electron
779 density surface. In the case of ADP most positive electrostatic potential concentration was observed
780 on the benzene and naphthalene and in BPO benzene ring is highly active and it play an important
781 role in the activity of BPO, whereas the sites corresponding to peroxide atoms is slightly active. In the
782 case of efficacy of ADP+BPO, the absorption values of some of the specific bands of biomolecules
783 present in the hair samples viz., protein, lipids, and squalene both the pre- and post-treatment subjects
784 were observed as biomarkers are significantly different between pre- and post-treatment hair samples
785 of acne patients. Some of the biomarkers such as $R1 = I_{3264/2864}$, $R2 = I_{1633/2864}$, $R3 = I_{1516/2864}$, and $R4$
786 $= I_{1454/2864}$ were used as diagnostic parameters, and hence the efficacy of Adapalene 0.1% and Benzoyl
787 Peroxide 2.5% is estimated. There is a significant difference between pre and post treatment ($P < 0.05$,
788 $P = 0.000$), there was no significant difference between healthy and post treatment acne patients ($P > 0.05$,
789 $P = 0.4290, 0.6040, 0.6160, 0.5070$).

790

791 Acknowledgment

792 The authors are thankful for the generous support Sophisticated Analytical Instrumentation
793 Facility (SAIF-SPIHER), St. Peter's Institute of Higher Education and Research, Avadi, Chennai-
794 600054, for permitting to deploy the advanced instrumentation FTIR-ATR technique.

795

796

797 REFERENCES

- 798 [1] Burton, J.L.; Cunliffe, W.J.; Stafford, I.; Shuster, S.; The prevalence of acne vulgaris in
799 Adolescence. *Br. J. Dermatol*: 2010; pp. 85:119-126.
- 800 [2] Ghodsi, S.Z.; Orawa, H.; Zouboulis, C.; Prevalence, severity, and severity risk factors of
801 acne in high school pupils: a community-based study. *J. Invest. Dermatol*: 2009; Volume
802 129, pp. 2136-2141.
- 803 [3] Plewig, G.; Dressel, H.; Pflieger, M.; Michelsen, S.; Kligman, A. M.; Low-dose isotretinoin
804 combined with tretinoin is effective to correct abnormalities of can. *J Dtsch Dermatol Ges*:
805 2004; Volume 4, (2), pp. 31-45.
- 806 [4] Stephen Titus and Joshushus Hodge., *Diagnosis and Treatment of Acne*, Fort Belvoir
807 Community Hospital Family Medicine Residency, Fort Belvoir, Virginia, 2012.
- 808 [5] Amichai, B.; Shemer, A.; Grunwald, M.H.; Low-dose isotretinoin in the treatment of acne
809 vulgaris, *J Am Acad Dermatol*: 2006; Volume 54, pp. 44-6.
- 810 [6] Hermes, B.; Praetel, C.; Henz, B.M.; Medium dose isotretinoin for the treatment of acne, *J*
811 *Eur Acad Dermatol Venereol*: 1998; Volume 11, pp.117-21.
- 812 [7] Strauss, J.S.; Leyden, J.J.; Lucky, A.M.; Looking bill, D.P.; Drake, L.A.; Hanifin, J.M.; A
813 randomized trial of the efficacy of a new micronized formulation versus a standard
814 formulation of isotretinoin in participants with severe recalcitrant nodular acne, *J Am*
815 *Acad Dermatol*,: 2001; Volume 45, pp.87-95.
- 816 [8] Akman, A.; Durusoy, C.; Senturk .M .; Koc ,C.K .; Soyturk D, Alpsoy E, Treatment of acne
817 with intermittent and conventional isotretinoin, A randomized, controlled multicenter

- 818 study, *Arch Dermatol Re*: 2007; Volume 299, pp. 467–73.
- 819 [9] Sardana, K.; Garg, V.K.; Sehgal, V.N.; Mahajan.; Bhushan, P.; Efficacy of fixed low-dose
820 isotretinoin (20 mg, alternate days) with topical clindamycin gel in moderately severe
821 acne vulgaris, *J Acad Dermatol Venereo*: 2009; Volume 23, pp. 556–60.
- 822 [10] Bowe, W.P.; Shalita, A.R.; Effective over-the-counter acne treatments, *Semin Cutan Med.*
823 *Surg* : 2008; Volume 27, pp. 170–176.
- 824 [11] Zouboulis, C.; Martin, J.P.; Update and future of systemic acne treatment, *Dermatology*:
825 2003; Volume 206, pp. 37–53.
- 826 [12] Korkut, C.; Piskin, S.; Benzoyl peroxide, adapalene, and their combination in the treatment
827 of acne vulgaris, *J Dermatol*: 2005; Volume 32, pp. 169–73.
- 828 [13] Ottaviani, M.; et al., Peroxidated squalene induces the production of inflammatory
829 mediators in HaCaT keratinocytes: a possible role in acne vulgaris, *J. Invest. Dermatol.* 2006;
830 Volume 126, pp.2430–2437.
- 831 [14] Smith, R.N.; Braue, A.; Varigos, G.A.; Mann, N.J.; The effect of a low glycemic load diet on
832 acne vulgaris and the fatty acid composition of skin surface triglycerides, *J. Dermatol. Sc*:
833 2008; Volume 50, pp.41–52.
- 834 [15] Borgfeldt, W.F. ;The evolving role of retinoids in the management of utaneous conditions,
835 *Clinician* 1998, Volume 6, pp.1–32.
- 836 [16] Ellis, C.N.; Millikan, L.; Smith, E.B.; Chalker, D.M.; Swinyer ,L.J.; Katz, I.H.; Berger, R.S.;
837 Mills, O.H.; Jr, Baker, M.; Verschoore .; Loesche ,C.; *Br J Dermatol*: 1998; Volume 139,
838 pp. 41-7.
- 839 [17] Thiboutot, D.; Gold, M.; Jarrattm, M.T.; Kang, S.; Kaplan, D.L.; Millikan, L.; Wolfe, J. C.;
840 Loesche ,C.; Baker, M.; *Cutis*: 2001; Volume 68, (4), pp. 10-9.
- 841 [18] Bershad, S.; Kranjac, G.; Singer Parente, J.E.; Tan, M.H.; Sherer, D.W.; Persaud, A.N.;
842 Lebwohl, M.; *Arch Dermatol*: 2002; Volume 138 (4), pp.481-9.
- 843 [19] Do Nascimento, L.; Guedes, A.C.; Magalhães ,G.M.; de Faria ,F.A.; Guerra, R. M.; de C
844 Almeida, F.J, *Dermatology Treat*: Sep 2003; Volume 14(3), pp.166-71.
- 845 [20] Millikan, L. E.Adapalene,an update on newer comparative studies between the
846 various retinoids, *Int J Dermatol*: 2000; Volume 39 (10), pp. 784-8.
- 847 [21] Korkut, C.; and Piskin, S.; Benzoyl peroxide, adapalene, and their combination in
848 the treatment of acne vulgaris, *J Dermatol*: 2005; Volume 32, pp.169–73.
- 849 [22] Ioannides, D.; Rigopoulos, D.; Katsambas .A.; Topical adapalene gel 0.1% vs.
850 isotretinoin gel 0.05% in the treatment of acne vulgaris: a randomized open-label
851 clinical study. *Br J Dermatol*: 2002; Volume 147, pp. 523–27. [PubMed]
- 852 [23] Dosik, J.S.; Homer, K.; and Arsonnaud, S.; Cumulative irritation potential of adapalene
853 0.1% cream and gel compared with tretinoin microsphere 0.04% and 01%. *Cutis*: 2005;
854 Volume 75, pp. 238-243.
- 855 [24] Brand,B. ;Gilbert, R.; Baker, M.D.; et al. Cumulative irritancy comparision of adapalene
856 gel 0.1% versus other retinoid products when applied in combination with topical
857 antimicrobial agents. *J.Am Acad Dermatol*: 2003; Volume 49, pp. S227-32.
- 858 [25] Frisch, M. J.;Trucks, G. W.; Schlegel, H. B.; et al., Gaussian 09, Revision, Gaussian, Inc ,
859 Walling Ford CT, 2009.

- 860 [26] Zhurko, G.A.; and Zhurko, D.A.; Chemcraft Program, J.; *Acta Crystallogr. Sect. E:*
861 *Structure*, 2004.
- 862 [27] Silverstein, M.; Clayton Basseler, G.; Moril, C.; *Spectro metric identification of org Compounds,*
863 *2nd,Edn*, Wiley, New York, 1981.
- 864 [28] Silverstein, R .M.; Calyton Bassler, G.; Tereence, C.; Morill, *Spectrometric Identification Of*
865 *Organic Compounds*, 5th (Ed), John Wiley & Sons, 1991.
- 866 [29] Plewig, G.; and Kligman, A. M.; *Acne and Rosacea_3 ed.*, Springer Science & Business
867 Media, pp. 613, 2012.
- 868 [30] Mulliken, R. S.; A new electroaffinity scale, Together with data on valence states and on
869 valence ionization potentials and electron Affinities, *J. Chem. Phys:* 1934; Volume 2,
870 pp. 782-793.
- 871 [31] Lukovits, I.; Bako, I.; Shaban and Kalmam, E.; Polynomial model of the inhibition-
872 mechanism of thiourea derivatives, *Electrochim.Acta*, 1998; Volume 43, pp. 31-136.
- 873 [32] Parr, R.G.; Szentpaly, L.V.; and Liu, S.; Electrophilicity index, *J.Am.Chem.Soc:* 1999;
874 Volume 121, pp. 1922- 1924.
- 875 [33] Lewis, R.J.; Sr (Ed.), *Hawley's Condensed Chemical Dictionary*, 12th ed. New York, NY:
876 Van Nostrand Rheinhold Co, 1993, pp.133.
- 877 [34] Ralf S Muller, In small Animal Clinical Pharmacology,(second Edition),Topical
878 dermatological therapy,2008.
- 879 [35] Tanghetti, E. A.; and Papp, K. F.; A current review of topical benzoyl peroxide: new
880 perspectives on formulation and utilization, *Dermatol clin*, 2009. [PubMed]
- 881 [36] Del Rosso, J.Q.; Leyden, J.J.; and Thiboutot D.; et al., Antibiotic use in cane vulgaris and
882 rosacea: clinical considerations and resistance issues of significance to dermatologists,
883 *Cutis:* 2008; Volume 82(2S), pp. 5–12[PubMed].
- 884 [37] Langner, A.; et al , Arandomized, single –blindcomparison of topical clindamycin +
885 benzoyl peroxide and adapalene in the treatment of mild to moderate facial acne vulgaris,
886 *Br J Dermatol*, 2008; Volume 159(2), pp. 480-1.
- 887 [38] Becke ,A.D.; *J.Chem.Phys:* 1993; Volume 98, pp. 5648-5655
- 888 [39] Lee, C.; Yang, W.; Parr, G.R.; *Phys.Rev :* 1988; B, Volume 37, pp. 785-793.
- 889 [40] Scorates, G. *Infrared and Raman characteristic group frequencies (tables and charts).*
890 *Chichester*, Wiley, 2001.
- 891 [41] Bellamy, L.I.; et al. *Z Elektrochim:* 1960; Volume 64, pp. 563-560.
- 892 [42] Dani VR, *Organic spectroscopy*, New Delhi, Tata MCGraw Hill, 1995.
- 893 [43] Sajan, D.; Josepha, L.; Vijayan, N.; Karabaca.; *Spectrochim.Acta A:* 2011; Volume 8,
894 pp. 85-98.
- 895 [44] Cieplak, P.; *J Comp Chem :* 1991; Volume 12, pp.1232.
- 896 [45] Chidangil, S.; Shukla, M. K.; and Mishra, P. C.; *J Mol Model:* 1998; Volume 4, pp. 250.
- 897 [46] Pepe, G, Siri, D.; Reboul, J .P.; *J Mol Struc (Theochem):* 1992; Volume, pp. 256:175.
- 898 [47] Anubha Srivastava, Poonam Tandon, Ayala, A .P. and Sudha Jain, *Vib Spec:* 2011;
899 Volume 56, pp. 82.
- 900 [48] Sankari, G.; Krishnamoorthy, E.; Jayakumaran, S.; Gunasekaran, S.; VishnuPriya, V. ;
901 Shyama, Subramaniam, S.; Surapaneni Krishna Mohan, Analysis of serum
902 Immunoglobulins using Fourier transform infrared spectral measurements, *J. Biology and*

- 903 *Medicine*: 2010; Volume 2, pp. 42-48.
- 904 [49] Akhtar, W.; Edwards HGM, Farwell DW, Nutbrown, M.; Fourier –Transform Raman
905 Spectroscopic study of human hair, *Spectrochimica Acta Part A*: 1997; Volume 53 ,
906 pp. 1021-1031.
- 907 [50] Tu, A.T, Raman spectroscopy in Biology: Principles and applications, *John Wiley and Sons*
908 1982.
- 909 [51] Chen, Y.J.; Cheng, Y.D.; Liu, H.Y.; Lin, P.Y.; Wang, C.S.; Observation of biochemical
910 imaging changes in human pancreatic cancer tissue using Fourier-transform infrared
911 microspectroscopy, *Chang Gung, Med J*: 2006; Volume 29, pp. 518-27.
- 912 [52] Barton, P.A.; Forensic Taphonomy Investigation of Single α -Keratin Fibres Under
913 Environmental Stress Using A Novel Application of Ftir-Atr Spectroscopy of Chemetrics,
914 Honours Thesis, Queensland University of Technology 2004.
- 915 [53] Bantignies, L.; Fushs, G.; Carr, G .L.; Williams, G .P.; Lutz, D.; Marull, S.. Organic Reagent
916 Interaction with Hair Spatially Characterized By Infrared Microspectroscopy, Using
917 Synchrotron Radiation, *Int Cosmet Sci*: 1998; Volume 20, (38), pp.94.
- 918 [54] Ottaviani, M.; Emanuela Camera, and Mauro Picardo. Lipid Mediators in Acne, *Mediators*
919 *of Inflammation*: 2010; pp. 858176-6.
- 920 [55] Zeyad El-Akawi, Nisreen Abdel-Latif, Khalid Abdul-Razzak, Mostafa Al-Aboosi, The
921 Relationship between Blood Lipids Profile and Acne, *Journal of Health Science*: 2005;
922 Volume 53, pp. 596-599.
- 923 [56] Boudiaf Boussouira and Dang Man Pham. Springer International Publishing Switzerland
924 G.T Wondrak (ed.), *Skin Response Pathways*, L' Oreal Research and Innovation, 88, rue
925 Paul Hochart, Chevilly Larue, France, 2016.
- 926 [57] Saint-Leger, D.; Bague, A.; Cohen, E.; Chivot, M.; A possible role for squalene in the
927 pathogenesis of acne, II. In vitro study of squalene oxidation, *Br J Dermatol*: 1986; Volume
928 114, pp. 535-42.
- 929 [58] Arora, M.K.; Seth, S.; Dayal, S.; Trehan, A.S; Seth, M.; Serum Lipid Profile in Female
930 Patients with Severe Acne Vulgaris, *Clin Lab*: 2014; Volume 60 (7), pp.1201-5.
- 931
- 932